CAPITAL UNIVERSITY OF SCIENCE AND TECHNOLOGY, ISLAMABAD

Screening of Active Constituents of *Artemisia absinthium* Against Mpro/PL2pro of HCoV-HKU1

by

Sobia Noureen

A thesis submitted in partial fulfillment for the degree of Master of Science

in the

Faculty of Health and Life Sciences
Department of Bioinformatics and Biosciences

2024

This thesis is dedicated to my dear and supportive family and friends who have fully helped me in achieving my life goals.

CERTIFICATE OF APPROVAL

Screening of Active Constituents of *Artemisia absinthium* Against Mpro/PL2pro of HCoV-HKU1

by

Sobia Noureen

(MBS221012)

THESIS EXAMINING COMMITTEE

S. No.	Examiner	Name	Organization
(a)	External Examiner	Dr. Sara Mumtaz	NUMS, Rawalpindi
(b)	Internal Examiner	Dr. Asad Anwar	CUST, Islamabad
(c)	Supervisor	Dr. Erum Dilshad	CUST, Islamabad

Dr. Erum Dilshad
Thesis Supervisor
April, 2024

Dr. Mariam Bakhtiar
Head
Dept. of Bioinfo. and Biosciences
April, 2024

Dr. Sahar Fazal
Dean
Faculty of Health and Life Sciences
April, 2024

Author's Declaration

I, **Sobia Noureen** hereby state that my MS thesis titled "**Screening of Active Constituents of *Artemisia absinthium* Against Mpro/PL2pro of HCoV-HKU1**" is my own work and has not been submitted previously by me for taking any degree from Capital University of Science and Technology, Islamabad or anywhere else in the country/abroad.

At any time if my statement is found to be incorrect even after my graduation, the University has the right to withdraw my MS Degree.

(Sobia Noureen)

Registration No: MBS221012

Plagiarism Undertaking

I solemnly declare that research work presented in this thesis titled "**Screening of Active Constituents of *Artemisia absinthium* Against Mpro/PL2pro of HCoV-HKU1**" is solely my research work with no significant contribution from any other person. Small contribution/help wherever taken has been duly acknowledged and that complete thesis has been written by me.

I understand the zero tolerance policy of the HEC and Capital University of Science and Technology towards plagiarism. Therefore, I as an author of the above titled thesis declare that no portion of my thesis has been plagiarized and any material used as reference is properly referred/cited.

I undertake that if I am found guilty of any formal plagiarism in the above titled thesis even after award of MS Degree, the University reserves the right to withdraw/revoke my MS degree and that HEC and the University have the right to publish my name on the HEC/University website on which names of students are placed who submitted plagiarized work.

(Sobia Noureen)

Registration No: MBS221012

Acknowledgement

All praise and thanks to the Supreme God to whom we only bow down. I also want to thank my family and friends for their unwavering prayers and support, both mentally and physically. I would also wholeheartedly say a big thank you to my supervisor Dr. Erum Dilshad (Associate Professor, Department of Bioinformatics and Biosciences, CUST) for her support with that I would say special thanks to Mr. Maaz (PhD Scholar) for giving his precious time to assist with computational approaches.

Thanks to all.

(Sobia Noureen)

Abstract

Respiratory illnesses ranging from mild to severe are commonly associated with human coronaviruses (HCoV). Notably, over the past 15 years, two highly infectious strains, the severe acute respiratory syndrome coronavirus (SARS-CoV) and the Middle East respiratory syndrome coronavirus (MERS-CoV), have emerged within the HCoV family. The replication process of these coronaviruses is tightly regulated due to variations in host factors and their adaptability to alter cellular and physiological structures. In the context of HCoV infections, the activation of specific signaling pathways triggers immune responses, affecting antiviral activities and ultimately amplifying the virus's pathogenesis. To mitigate disease spread, various strategies, such as repurposing drugs and implementing measures like sanitization, social distancing, and mask-wearing, have been deployed. The global scientific community has been dedicatedly exploring solutions to combat these viruses, including researching natural compounds from plants. A detailed investigation into HCoV-HKU1 revealed a potential target in the non-structural protein Mpro/PL2 pro, responsible for cleaving replicating enzymes. One active compound found in *Artemisia absinthium* underwent studies to ascertain its efficacy against Mpro and PL2pro. Fifteen ligands from diverse classes were chosen and screened based on Lipinski Rule and ADMET properties. Following the docking process using CB dock, chrysoplenetin emerged as a lead compound compared to the standard drug Remdesivir. The docking results, visualized through PyMol and analyzed via LigPlot, suggested that chrysoplenetin might exhibit higher effectiveness against Mpro/PL2pro compared to Remdesivir. However, further comprehensive research is imperative to explore the potential medicinal utility of chrysoplenetin in combating HCoV infections.

Contents

List of Figures

List of Tables

Abbreviations

A. absinthium	*Artemisia absinthium*
ACE	Angiotensin-converting enzyme
BBB	Blood-brain barrier
CNS	Central Nervous System
FDA	Food Drug Authority
Mpro	Main protease
PLP	Papain like Protease
PDB	Protein Data Bank
RNA	Ribonucleic acid
SARS	Severe acute respiratory syndrome
MRTD	Maximum rate tolerated dose
OCT	Organic cation transporter

Chapter 1

Introduction

Human coronavirus HKU1 (HCoV-HKU1) is a particular type of coronavirus that primarily infects animals and humans. Symptoms caused by this coronavirus include upper respiratory diseases similar to common cold symptoms, often leading to pneumonia and bronchiolitis [1]. It was first identified in January 2004 when a man in Hong Kong contracted the virus [2]. This disease affecting the lower respiratory tract leads to approximately 4 million deaths worldwide annually. Various viruses, like influenza virus, respiratory syncytial virus (RSV), and parainfluenza virus, are known to cause respiratory tract infections. However, in a considerable number of respiratory tract illnesses, no specific pathogen is identified [3].

Under an electron microscope, coronavirus virions typically exhibit pleomorphic or spherical shapes, with particles measuring about 80–120 nm in diameter. The surface of these coronavirus particles is decorated with club-like projections of the spike (S) protein. In certain beta coronaviruses, like HCoV-OC43 and HCoV-HKU1, short hemagglutinin-esterase (HE) protein projections have also been observed. The outer viral envelope contains a small amount of the envelope (E) protein, which is primarily maintained by the membrane (M) protein. The nucleocapsid (N) protein, when adhering to the DNA inside the viral envelope, forms a helical, symmetric nucleocapsid [4]. Typically, the receptor targeted by this virus is 9-O-acetylated sialic acid. HCoV-HKU1, like other coronaviruses, likely possesses its main protease (M^{pro}), also known as a 3C-like protease, and papain-like

protease (PLpro or CLpro). These proteases play crucial roles in processing and producing viral polyproteins during the viral replication cycle. However, the specific proteases in HCoV-HKU1 and their functions may not have been extensively characterized compared to more pathogenic coronaviruses [4, 5].

Respiratory disorders worldwide are predominantly caused by coronaviruses like HCoV-229E and OC43, while SARS-CoV, HCoV-HKU1, and MERS-CoV pose significant threats to public health. Despite the approval of various vaccines to protect against animal coronaviruses and the development of promising vaccine platforms for SARS-CoV in preclinical studies and trials, there are currently no FDA-verified vaccines specifically designed to treat human coronavirus infections [6]. Several vaccines are under development, each with distinct treatment regimens. Initially, the elderly were prioritized for vaccination, yet transmission persisted. Subsequently, vaccinating the younger population led to a decrease in positive cases. However, diverse vaccination strategies tailored to demographic regions, virus transmission, and mutations remain essential to prevent and mitigate the virus's impact [7].

In pursuit of new strategies for medicinal development against human coronaviruses, research has focused on natural compounds with documented potent antiviral and anti-inflammatory properties. M^{pro}, identified as a potential drug target, exhibits effective binding affinity with specific antiviral and anti-inflammatory compounds. Over the last thirty years, computer-assisted drug discovery and design methods have played a crucial role in therapeutic medicine development [8]. Computational methodologies like molecular docking have proven beneficial, reducing costs and time required to identify potential drug candidates, surpassing manual methods in speed [9].

Historically, medicinal plants have been utilized to combat various viral diseases. Efforts have been made to isolate small molecules from plants demonstrating inhibitory activity against viruses. Genomic sequencing has indicated similarities between medicinal plants effective against HCoV-HKU1 and SARS-CoV-2, especially in targeting PL2pro as a potential site. Therefore, for this virus, the

main protease serves as a screening target against active compounds derived from medicinal plants [10].

1.1 Problem Statement

Human coronaviruses (HCoVs), are commonly responsible for causing the common cold with minimal clinical effects [11]. To combat this, it's crucial to discover and identify new compounds with potent antiviral properties, minimal side effects, and global accessibility, aiming to reduce the impact of the virus. This study focuses on targeting the main protease (M^{pro})/PL2pro enzyme of the virus using active compounds with antiviral properties found in *Artemisia absinthium*. Extensive computational studies through molecular docking have been conducted as part of this investigation.

1.2 Aim and Objectives of Study

The main aims of this study is to predict potential inhibitors against HCoV-HKU1 by the use of molecular docking of active compounds of *Artemisia absinthium* showing antiviral properties against M^{pro}/PL2pro of HCoV-HKU1 to control disease caused by the virus.

The objectives of the study include:

1. To identify the probable inhibitory compounds with antiviral properties present in *Artemisia absinthium* against the main protease of HCoV-HKU1.
2. To examine the interactions between ligands and proteins complex by performing molecular docking.
3. To find the best of the interacting molecules that show inhibitory effects against the virus main protease, M^{pro}/PL2pro.

Chapter 2

Literature Review

The newly evolved human coronavirus HKU1 (HCoV-HKU1) was first reported in Hong Kong in 2005. The main infection caused by HCoV-HKU1, which occurs around the world results in symptoms such as bronchitis, the common cold and pneumonia. The CoV main protease (Mpro), which is an important enzyme help in replication of virus via the proteolysis the replicase polyproteins, has been identified as an appealing target for logical drug development [12]. The coronavirus virions seem polymorphic or physiologically spherical when noticed under an electron microscope. Typically, the 80–120 nm-diameter enveloped coronavirus particles have club-like extensions of the spike (S) protein adorning their surface. It has also been shown that certain beta coronaviruses, such as HCoV-OC43 and HCoV-HKU1, have brief extensions of the hemagglutinin-esterase (HE) protein. A relatively small amount of the envelope (E) protein exists in the viral envelope, which is sustained by the membrane (M) protein. The nucleocapsid (N) protein binds the DNA inside the viral envelope to create a helical symmetric nucleocapsid. Coronaviruses have an envelope that surrounds the viral particle. This envelope is derived from the host cell membrane as the virus exits the host cell. It contains various viral proteins, including the spike (S) protein, which is responsible for binding to host cell receptors and is a significant target for the host's immune response. The spike protein is a large glycoprotein that protrudes from the viral envelope. It plays a critical role in binding to host cell receptors and facilitating virus entry into host cells. The S protein is also the primary target of antibodies

and is used in the development of vaccines. Inside the envelope, the coronavirus genome is tightly packed with nucleocapsid proteins. The N protein binds to the viral RNA and helps shape the viral particle. It is involved in viral replication and assembly. The M protein is a structural protein that helps give the virus its shape. It interacts with the nucleocapsid and the envelope, providing structural integrity to the viral particle [13].

The E protein which is usually small but integral membrane protein that plays vital role in assembly of virus and its release. It is also involved in viral pathogenesis. The coronavirus genome is a usually single-stranded positive RNA molecule which usually carries the important genetic information for replication of virus and expression of proteins of viruses. So far, about 22 HCoV-HKU1 genomes have been sequenced [13]. The genomes of HCoV-HKU1 vary in size, including 29,295 to 30,097 nucleotides. When it comes to G + C content, the HCoV-HKU1 genomes have the lowest of all known coronaviruses whose whole genome sequences are available, at about 32%. The HCoV-HKU1 genome shares the same gene order 5'-replicase ORF1a,b, spike (S), envelope (E), membrane (M), and nucleocapsid (N)-3' with other coronaviruses. This arrangement makes the genome mostly comparable to other coronaviruses (Figure 2.1) [14].

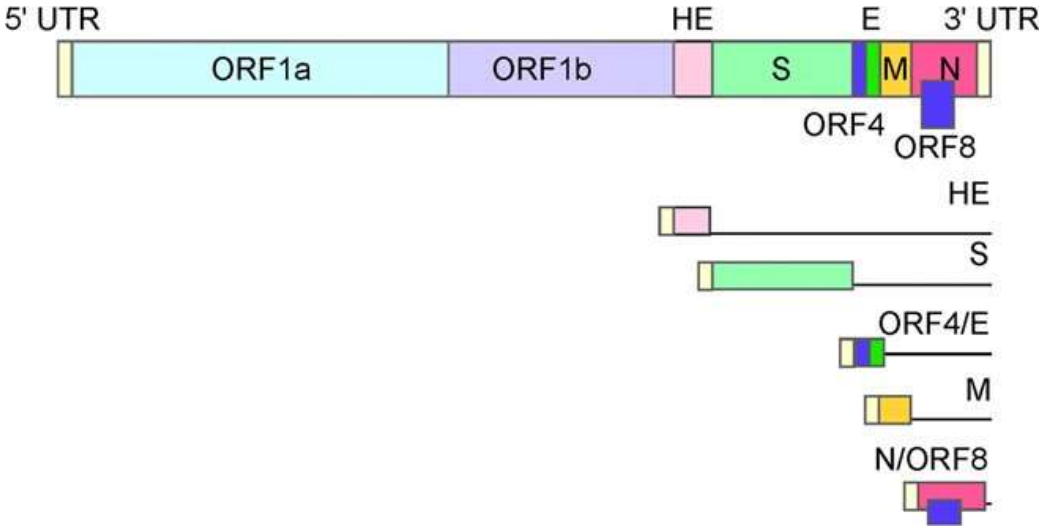

FIGURE 2.1: Structure of HCoV-HKU1 [14]

2.1 Origin

With the emergence of the human coronavirus, many questions related to its evolution, introduction of the virus in the human race, reservoirs of the virus, spread of the virus,the linkage of the animal virus with its effects on humans and certain other matters were raised. After obtaining the genomic sequence of the virus, it was aligned with the available data in databases with the use of BLASTn to find the homology of this virus. The human coronavirus strain HKU1 that has been found here has been deposited in GenBank with accession codes MH940245 and PRJNA509533 [14].

Upon transcription, the beta coronaviruses produce almost 800KD polypeptide. The polypeptide is cleaved by papain like protease and 3-chymotrypsin like protease to generate various non-structural protein involved in viral replication [14].

2.2 Entry and Life Cycle

The replication cycle, which makes up the HCoV life cycle, contains five phases: The first stage of the virus's life cycle involves attachment to the host cell, intracellular envelopment, uncoiling, replicase expression, replication-transcription complex formation, RNA synthesis, and virion discharge. The binding of coronavirus virions to host cell receptors usually begins the infection phase. The S protein, which has two functional domains, is composed of the S1 (bulb), which attaches to receptors, and the S2 (stalk), which connects cell membranes with virion. Modifications occur in the receptor-binding domain (RBD) of S1 between coronaviruses. The RBDs of HCoV-229E, HCoV-NL63, and HCoV-HKU1 are found in the C-terminal domains of their respective S1 subunits, but not in the N-terminal domains. Receptor binding usually starts the virus infection. HCoV usually utilizes receptors present on the cell membrane, which are cellular proteins or carbohydrates. It's interesting to take into account that each protein receptor for HCoV that is known at present occurs on the cell surface. Some of these receptors include angiotensin converting enzyme 2 (ACE2) for HCoV-NL63,

SARS-CoV, and SARS-CoV-2, aminopeptidase N (APN) for HCoV-229E, and dipeptidyl peptidase 4 (DPP4) for MERS-CoV. On the other hand, glycan-based receptors expressing 9-O-acetylated sialic acid are employed by HCoV-OC43 and HCoV-HKU1. The Figure 2.2 shows the Entry and life cycle of the HCoV-HKU1 in human cell [15].

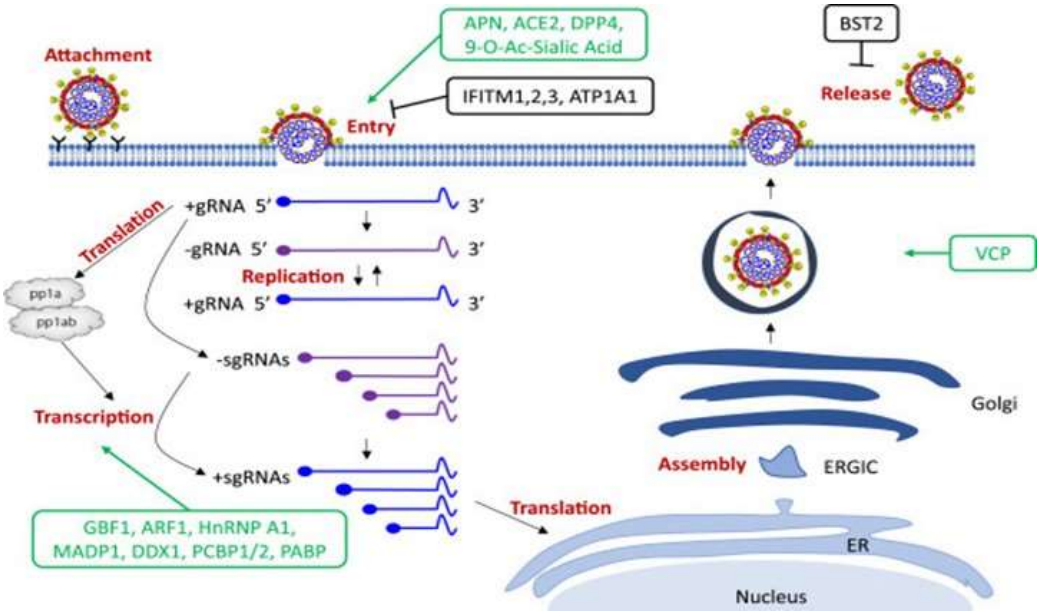

FIGURE 2.2: Entry and life cycle of the HCoV-HKU1 in human cell [15]

2.3 Symptoms

Examining the symptoms that those afflicted with HCoV, RSV, and influenza had been reported. It is statistically significant that there are no variations in the frequency of vomiting, diarrhea, red throat, and rhinitis instances amongst all viruses. In addition, HCoV infections have been reported to have a similar or lower incidence of all symptoms when compared to influenza infections. Relative to both influenza and RSV, fewer patients with HCoV reported fever. Compared to HCoV patients, a greater percentage of influenza-positive individuals may have suffered shaking, migraines, fatigue, and joint and muscular pain. Fever, cough, and dyspnea were less common in HCoV-infected patients compared to RSV-infected

patients; however, HCoV-infected patients were more likely to suffer symptoms such as headache, fatigue, muscle discomfort, shaking, and sore throat.

However, the additional illnesses leading to infection of upper respiratory tract were not found (e.g., hPIV, hMPV, rhinovirus, adenoviruses, and bocaviruses) [16].

2.4 Treatment for Human Corona Virus HCoV

However, there haven't been many studies on antiviral therapy for coronaviruses besides SARS-CoV. Research studies for the treatment of infections caused by HCoV-HKU1 have not been performed. The limited in vitro data suggests that HCoV-NL63 may be suppressed by intravenous immunoglobulins, heptad repeat 2 peptide, siRNA, and other compounds. Furthermore, HCoV-229E may be suppressed by saikosaponins, a class of oleanane derivatives obtained from particular botanical species [17].

Ribavirin

During the 2003 epidemic, ribavirin a synthetic nucleoside, was used exclusively to treat HCoV patients. Several clinical studies have been carried out, including a retrospective case series and one that determined the effectiveness of ribavirin in treating HIV patients after different clinical arms of randomized clinical trials. However, a conclusive resolution was not possible later on 40% of the 144 patients in the Greater Toronto study had transaminases that were elevated by 1.5 times, over half of the patients had hemoglobin reductions (>2 g/dl), and 126 of the patients got high dosages of ribavirin [18].

2.5 Medicinal Plants

Medicinal plants are those that have shown therapeutic properties and have shown beneficial results on humans and animals. They have been used since early times

for the treatment of different diseases. In early times with their instincts, taste and smell abilities humans used different plants. Some plants were directly applied to injuries, some were boiled to extract the components present in that plant for treatment. For this the therapeutic properties of many plants have been under consideration and these plants have been used as an important source for lead drugs [19].

Since the first spread of the virus, individuals have been treated with herbal medicines. Early 90% of the individuals were recovered by the use of herbal medicines. Some of the remedies prevented the spread of HCoV in individuals and other remedies have treated the symptoms of the disease from an acute to severe level [20].

Therefore, the innovation of new antiviral drugs is an important issue because of life-threatening viral diseases such as Ebola, SARS, and MERS. Alot of plants have produced numerous phytochemicals with great potential in order to overcome these diseases. For example, Toona sinensis Reom, also referred to as *Cedrela sinensis*, family *Meliaceae*, is a tree that is frequently discovered in Taiwan, China, and Malaysia. Because of its potency against HCoV-229E, herbalists and specialists in Traditional Chinese Medicine (TCM) have described this tree's potential to produce multiple phenolic compounds and sterols. This plant's leaf extract suppressed SARS-CoV replication in vitro with a suppression index of 12–17 [17]. The potential of extracts from a few medicinal plants, such as *Paeonia suffruticosa Andrews* (Paeoniaceae), *Phellodendron amurense Rupr.* (Rutaceae), *Melia azedarach L.* (Meliaceae), *Cimicifuga racemosa (L.) Nutt.* (Ranunculaceae), and *Coptis chinensis Franch.* (Ranunculaceae) as anti-SARS-CoV candidates have been demonstrated through in vitro antiviral assays of some medicinal plant extracts [21].

For the inhibition of binding of spike protein of the virus to the ACE2 receptor ,141 medicinal plants and almost 49 natural compounds in their purified form was reported. These 16 already present drugs were reported to inhibit angiotensin type IA receptors in-vitro [22]. Many flavonoids were tested against the main protease for inhibitory effects.

2.6 *Artemisia absinthium*

Artemisia is the largest genera included in the family Asteraceae. The name Artemisia has been derived from the name of the Greek goddess Artemis, who was considered as protector of the wild. Another proposition about the name of the genus is from the name of the queen (Artemisia) of Cairo.

The 500 species of this genus is spread all over the world except for the extreme colds of Antarctica [23]. Absinthium, native to Europe, was introduced to North America in 1841. It is now naturalized across the northern United States and in Canada. It is an herbaceous plant as shown in Figure 2.3 [24]. This medicinal plant has been used as a part of dietary spice and as herbal tea.

The pharmacological characteristics and effects of a number of Artemisia species of the plants that have been collected from different parts of the world have been reported. Some common applications of this plant include memory improvement, respiratory and digestive problems, headaches, dyspepsia, liver and kidney tonic, anti-malarial, anti-spasmodic, anti-inflammatory, febrifuge, heart stimulant, anthelmintic, and hypertensive and anticoagulant illnesses [25]. *Artemisia absinthium* is rich in approximately 600 active metabolites of which *Artemisinin* and its derivatives are most commonly used.

Other metabolites such as terpenoids, sesquiterpenoids, monoterpenoids, couramins, flavonoids, alkaloids, triterprenoids, steroids, benzenoids and alkaloids are also of major interest [26].

Due to the presence of large metabolites, *Artemisia absinthium* has also shown antifungal, antitumor, hepatoprotective, anti-asthmatic and antioxidants properties. The plant is also rich in minerals, vitamins and essential amino acids making it an essential candidate for the food, pharmaceutical, nutraceutical, medical and cosmetic industries. The taxonomic hierarchy of *Artemisia absinthium* is given in the table 2.1 [27].

FIGURE 2.3: *Artemisia absinthium* [24]

TABLE 2.1: Taxonomic hierarchy of *Artemisia absinthium*

S.No.	Domain	Eukarya
1	Kingdom	Plantae
2	Clade	Tracheophytes
3	Clade	Angiosperms
4	Clade	Eudicots
5	Clade	Asterids
6	Order	Asterales
7	Family	Asteraceae
8	Genus	Artemisia
9	Specie	*A. Absinthium*

2.7 Molecular Docking

Molecular docking has been in use for the past three decades for designing drugs with computer assistance and to find different structures in molecular biology. Docking is preferred while performing virtual screening on the compounds present in the databases or libraries for analysis of their functions. Results can be classified easily through docking and one of the main roles played by docking is to give an analysis of how the ligand interacted with the protein, locking it for optimizing the lead compounds for drug development [28].

Different docking programs use either one or more search algorithms for the prediction of possible results of the receptor-ligand complex. This is the main reason

behind the rise in popularity of molecular docking as a vital tool in drug discovery and molecular modeling applications. The docking result gives a score for the interaction and the accuracy of the scoring function makes docking more reliable for predicting the ligand pose and through that the binding site of the ligand can also be determined. With this, it predicts the binding affiliation which in turn leads to the identification of a potential lead drug in association with the target protein [29].

2.8 Mpro/ PL2pro

The primary agents responsible for SARS-CoV infections, belonging to the family of human coronaviruses (HCoV), encompass HCoV-OC43 (β-CoV), HCoV-229E (α-CoV), HCoV-NL63, and HCoV-HKU1. Scientists exploring innovative anti-SARS-CoV-2 drugs have been guided by the strong phylogenetic resemblance between SARS-CoV-2 and HCoV-OC43, and HCoV-229E, both of which are major contributors to the common cold [30].

Notably, studies have shown similarities between the host receptor of SARS-CoV-2, angiotensin-converting enzyme 2 (ACE2), and that of SARS-CoV, suggesting that targeting ACE2 could be an effective approach in containing the pneumonia outbreak [31]. Prior research has emphasized the significance of utilizing medications that inhibit enzymes crucial in the replication of SARS-CoV, particularly the papain-like protease (SARS-CoV PLPro) and SARS-CoV 3C-like protease (SARS-CoV 3CLPro). These enzyme inhibitors play a pivotal role in hindering the expression of essential replicative enzymes like RNA-dependent RNA polymerase (RdRp) and helicase, thereby impeding viral replication [32].

Regarding the structural aspects, three distinct crystal structures of 3CLpro have been identified: the wild-type active dimer, monomeric forms incapable of dimerization (including G11A, S139A, and R298A mutants), and the highly active dimer. The catalytic domain spans residues 8 to 184, the N-terminal finger comprises residues 1 to 18, and the C-terminal domain encompasses residues 201 to 306 [33].

2.9 Natural Compounds as Inhibitors of PL2pro

The main protease (Mpro) of the virus which controls the replication process is considered an active site for targeting the drugs against the virus. The 3D structure of the enzyme is screened against the medicinal plant library with almost 32,297 phytochemicals that have shown antiviral properties. Three drugs Colistin, Nelfinavir and Prulifloxacin were shown to inhibit the enzyme by drug repurposing strategies. With that certain phytochemical like 5,7,3',4'-tetrahydroxy-2'-(3,3-dimethylallyl) which is a flavone has shown highest docking score against Mpro. This flavone is extracted from *Psorothamnus arborescens* Myricithin from the plant Myrica cerifera, Methyl rosemarinate from the plant *Hyptis atrorubens*, 3,5,7,3',4',5'-hexahydroxy flavanone-3-O-beta-D-glucopyranoside from the plant *Phaselous vulgaris*, Licoleafol from plant *Glycyrrhiza uralensis* and Amaranthin from plant *Amaranthus tricolor* were identified as inhibitors to Mpro [34].

From tetrapeptide inhibitor 3 serine derivatives were also screened for inhibitory effects. Herbacetin, pectolinarin and rhoifolin were also found to show inhibitory effects. Certain chalcones in alkylated form derived from Angelica Keiskei showed inhibition effects. The docking results showed that hydroxyl and carbonyl groups formed hydrogen bonds with Ser-144 and His-163 [35].

From the Zinc drug database 27 drugs were identified as potential inhibitors of $3CL^{pro}$. These drugs include lymecycline, chlorhexidine, alfuzosin, cilastatin, famotidine, almitrine, progabide, nepafenac, carvedilol, amprenavir, tigecycline, demeclocycline, montelukast, carminic acid, mimosine, Flavin mononucleotide, lutein, cefpiramide, phenethiacillin, candoxatrill, nicardipine, estradiol valerate, pioglitazone, conivaptan, telmisartan, doxycycline and oxytetracycline [36].

In natural product database certain compounds were also found to work against 3CLpro and these include compounds like 1-formamido, 6-methyldihydrofuran which were *Andrographodile* derivatives, beutonal which is derived from the plant Cassine xylocarpa, Isodecortinol, Cerevistirol both are derived from the plant *Viola diffusa*. Many other natural compounds from the plants like *Citrus aurantine*,

Scutellin baiclensis, *Phyllantus emblica*, *Ficus benjamina*, *Camellia sinensis*, *Swertia kouitchensis*, *Gnidia lamprantha*, *Swertia macrosperma* and many more plant derivatives have shown promising antiviral, anti-inflammatory activity against the main protease of HCoV [37, 38].

2.10 Inhibitors Against PL2pro of HCoV-HKU1 in *Artemisia absinthium*

There are large number of naturally occurring compounds that can serve as antivirals to inhibit the activity of main protease of HCoV. The natural compounds have shown minimal side effects with low toxicity and the important thing is they are easily available to a large mass. The plant *Artemisia absinthium* have been used from the earlier times either in the form of tea or in the form of juice for curing of malaria and other fevers. This was such a remarkable cure that this herb approximately 4.5-5g in dried weight was converted into an infusion for clinical trials [31].

Chapter 3

Materials And Methods

3.1 Selection of Disease

Human coronaviruses (HCoVs) are a group of viruses that primarily infect humans and can cause respiratory illnesses of varying severity. Common human coronaviruses include HCoV-229E, HCoV-NL63, HCoV-OC43, and HCoV-HKU1. These viruses typically cause mild respiratory infections, with symptoms like the common cold, cough, and sometimes fever. To control the transmission of this virus availability of the drugs has to be ensured. The main protease of HCoV-HKU1 is identified as to play vital role in the replication of the virus. For this purpose, it provides a potential site for drug targeting [17]. Though much work is done but the gaps still remain which needs to be filled.

3.2 Selection of Protein

The main purpose of selection of the respective protein is that it plays an important part in the life cycle of the virus. The PL2pro/Mpro plays a vital role in the cleavage of essential 11 sites in replicase polyproteins which releases certain enzymes that are needed for the replication of the respective virus [38]. The structure of HCoV-HKU1 PL2pro/ Mpro has been downloaded from the available resource

of protein data bank (PDB). With the DOI https://doi.org/10.1128/JVI.00298-08 and the P0C6U3and DOI https://doi.org/10.1128/JVI.00298-08 3D23 the crystal-like structure of the main protease of HCoV-HKU1 had been downloaded.

3.3 Determination of Physiochemical Properties of Proteins

The study and determination of the physiochemical properties of a protein have a key role in the finding of its function. ProtParam a tool of ExPAsy had been used for this purpose physiochemical properties like the molecular weight, isoelectric point, number of amino acids present, grand average of hydropathicity, instability index, number of negatively charged residues (Asp+ Glu) and positively charged residues (Arg+Lys) all can be studied.

3.4 Cleaning of the Downloaded Protein

After downloading the protein structure, the extra constituents attached to the protein needs to be removed which is done by the use of an open-source system Pymol. The linear chain of consisting of range 1-306 amino acids had been kept referring as the A chain and remaining all the constituents of the protein had been eliminated so that further process is done effectively [39].

3.5 Determination of Functional Domains of Target Proteins

For determining the domains of the target protein InterPro a database that can analyze a protein is used with that it also provides information regarding the families, functional sites and the domains of the protein under study [40]. By

inserting the FASTA sequence of the main protease we got the polypeptide binding sites and homodimer interfaces www.ebi.ac.uk/interpro/result/InterProScan/

3.6 Selection of Active Metabolic Ligands

Those ligands had been selected that have previously shown some antiviral and antimalarial properties. These includes the terpenes, monoterpenes, sesquiterpenes, phenolic compounds, flavonoids, coumarins and sterols [31].

3.7 Ligand Preparation

By using the database PubChem we had downloaded the 3-dimensional structure of the above selected ligands. PubChem is under the National Center of Biotechnology Information (NCBI) and is a database that contains the essential data regarding the chemical molecules. The information stored is related to the chemical names, molecular formulas. 3 dimensional or simple structures, their isomers, canonical similies and information regarding the activities of the molecules against the biological assays [41].

The structure of the ligands which are obtained from PubChem had been downloaded and then the ligands MM2 energy had been minimized by using Chem3D ultra. If in case the selected ligand structure is not available then our next attempt had to download the canonical similies from PubChem and then insert them in the software Chem Draw and after obtaining the 3D structure repeat the energy minimization step using Chem3D ultra. At the end pdb format had been selected to save the energy minimized structure of the ligand.

3.8 Molecular Docking

To carry out the protein and ligand molecular docking process, CB-dock (Cavity detection guided blind docking) had been used. CB dock finds the sites of docking

automatically. CB-Dock is a method of protein and ligand docking which indicates about the sites of bonding, the size and the center is calculated. The box size is adjusted according to the ligand and then docking is performed. The docking is performed through AutoDock Vina. As it is docking focused on cavity binding so ratio of accuracy is higher [42].

For performing the docking we will upload the 3D structure of protein in pdb format and the 3D structure of ligand in the sdf format. After this docking is performed. The end result would be 5 different poses of interaction. To select the best pose we would look upon the minimum vina score which is given in KJ/m-1 CB-Dock will provide an interactive 3D visualization of results in 5 different poses. Best pose had been selected on basis of minimum vina score given in (kJ/m-1) [33].

3.9 Visualization of Docking Result via PyMol

Over the past few years the PyMol had been emerged as an efficient molecular tool of visualization. The graphics and its ability to view 3D structures have been extraordinary [34]. PyMol provides a plugin which can access the results and make their visualization clearer so that the docking results can be easily studied. The pictures of the docking result can be captured also. For all the process the docking result had been be saved in the pdb format and after visualization in the PyMol it has been saved in the pdb file format.

3.10 Analysis of Docked Complex via LigPlot

Once we get the docked complex with the lowest vina score, the next step was the analysis of the complex. The complex had been in the pdb format. This analysis was done by using the software LigPlot. The protein and ligand interaction schematic designs have been automatically created for the specified pdb file format. Hydrophobic contacts and hydrogen bonding alter these interactions. The

study of hydrogen bonding and hydrophobic interactions is provided by LigPlot. With this LigPlot generates the 2D representation of the protein-ligand complex [43].

3.11 Ligand ADME Properties

After the analysis the next step was the study of pharmacokinetic and toxicity properties. The weak candidates of the drug had been eliminated during preclinical ADME. The remaining applicants may be chosen to test potential treatments for the disease. By using the PkCSM optimization of the ADME which is Absorption, Distribution, Metabolism and excretion related to human body had been done [44].

3.12 Lead Compound Identification

After all the work is performed the next step had been to find the lead compound. The lead compound is identified after applying the rule of 5 which includes:

1. The log value of the drug-like compound must be limited to 5.
2. The molecular weight should also be lesser than 500.
3. Hydrogen bond acceptors maximum number should be 10.
4. Hydrogen bond donors' maximum number should be 5.

Once the compound fulfills these rules it had been be selected as our lead compound. The selected compound is our lead compound [45].

3.13 Comparison with the Standard Drug

Remdesivir a drug which has shown antiviral properties against MERS, HCoV HKU1 and other viruses has been selected as a standard drug for comparison against the lead compound. Remdesivir had been used against proteins of viral

replication and has shown effective results when used in places like Rome and USA [46, 47].

3.14 Overview of Methodology

Overview of methodology opted for this study is shown in Figure 3.1

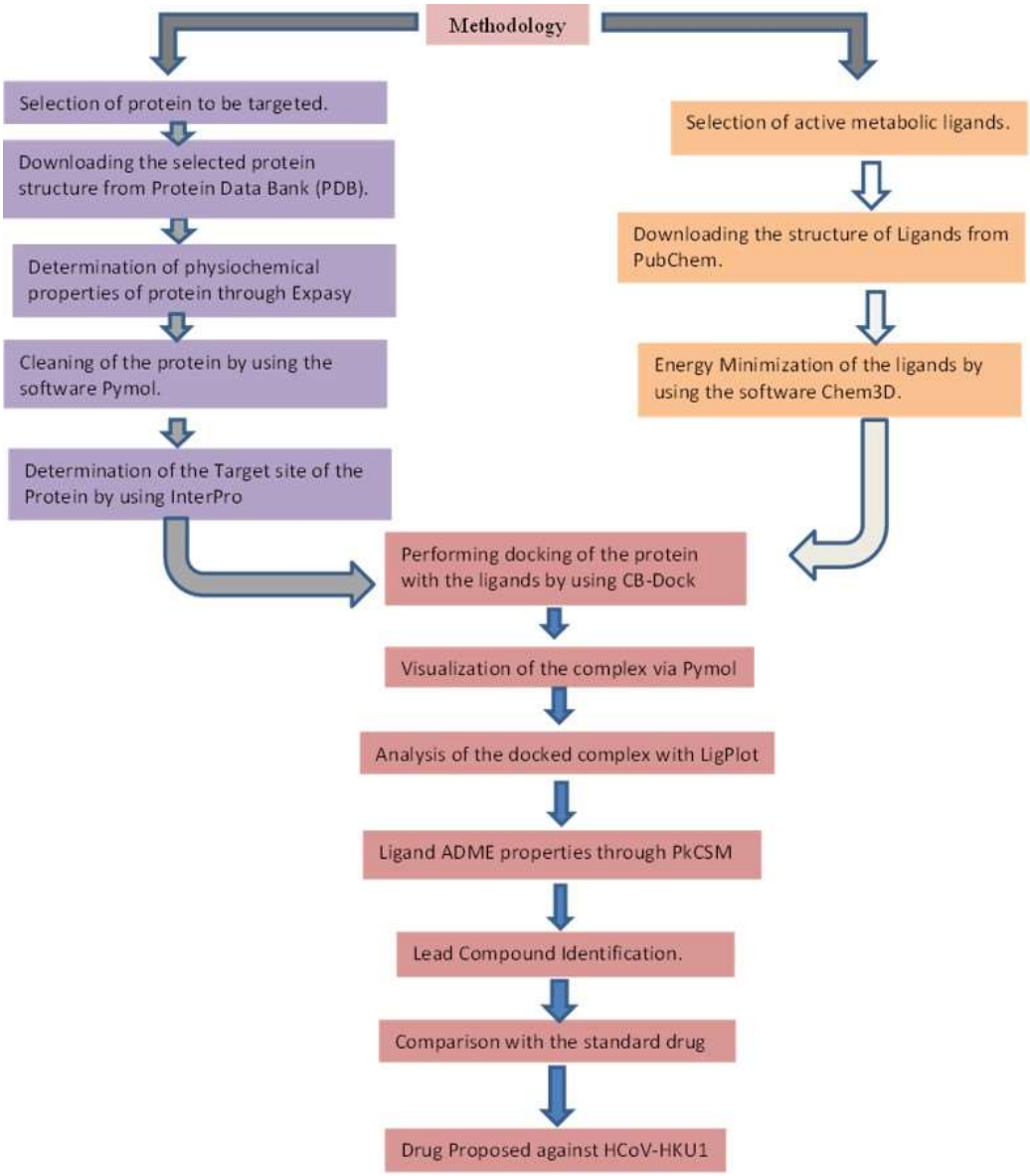

FIGURE 3.1: Overview of Methodology

Chapter 4

Results and Discussion

4.1 Structure Modelling

M^{pro} is selected as the target protein to act against the essential components present in *Artemisia absinthium*. The M^{pro} of the HCoV-HKU1 plays a major role in the cleavage of essential 11 sites in replicase polyproteins which releases certain enzymes that are needed for the replication of the respective virus [48].

4.1.1 3D Structure of the Protein

The chosen protein, M^{pro}, is an enzyme of the coronavirus that is essential for mediating the virus's transcription and replication. For this reason, it is considered as an attractive enzyme of the virus to be targeted. M^{pro} is a 33.8 kDa protein which digests the polyprotein at almost 11 conserved sites making it an efficient drug target [49]. The PDB (Protein Data bank) contains massive amount of information regarding the protein-ligand complexes. The 3D structure of the main protease of coronavirus was obtained from a protein data bank (PDB) named 3D23 with the DOI/10.2210/pdb3D23/pdb. The protein M^{pro} of HCoV-HKU1 as shown in Figure 4.1 was energy minimized for further processing.

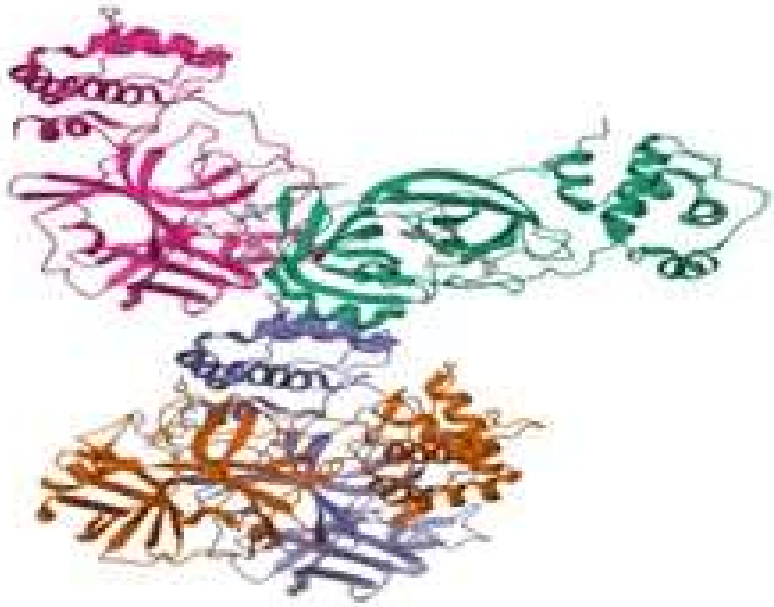

FIGURE 4.1: M^{pro} of HCoV-HKU1 [3D23]

4.1.2 Physical Properties of Protein

For studying the properties of protein M^{pro} a tool of ExPASy named as ProtParam is used. It is an online tool that is used for computing the physiochemical properties of proteins that are entered in the Swiss-prot or TrEMBL or for the proteins entered by the users. The parameters which are studied include the molecular weight, protein's amino acid composition, atomic composition, theoretical pI, estimated half-life, extinction co-efficient, instability index, aliphatic index, and the last is the grand average of hydropathicity (GRAVY) [50].

With this, the protein showing pI greater than 7 means the basic nature of the protein whereas a pI value lesser than 7 indicates the acidic nature of the protein. Extinction coefficient indicates the light absorption whereas instability index represents stability level of protein if it is lesser than 40 then that means the protein is stable any value greater than 40 shows that protein is unstable [50].

The aliphatic index shows the thermo-stability of a protein. The molecular weight (MW) of the protein shows both the positive and the negative amino acid residues.

NR indicates the negative residues (Asp+Glu) and PR represents the positive charge residues (Arg+Lys). The low GRAVY value shows the interaction with water molecules. All the above-mentioned parameters were taken into consideration [50].

TABLE 4.1: Physical Properties of M^{pro}

MW	**pI**	**NR**	**PR**	
451387.72	6.29	374	347	
Ext. Co 1	**Ext. Co 2**	**Instability Index**	**Aliphatic Index**	**GRAVY**
543705	534830	30.14	97.21	0.255

The above Table shows the molecular weight of M^{pro} as 451387.72 which is a collective weight of negative and positive amino acids residues. The pI is 6.29 which shows that the selected protein is acidic in nature.

The values of light absorption in terms of extinction coefficient is 543705 and 534830. The instability index value of 30.14 shows that selected protein M^{pro} is quite a stable protein. Aliphatic index also shows that selected protein is thermostable. Low value of GRAVY shows that M^{pro} has good interactions with water molecules.

4.1.3 Identification of Functional Domains of the Protein

For identifying the functional domains InterPro consortium is used. InterPro helps in finding the functional analysis of proteins and classifies them into families which is done by finding functional domains and other important sites. Functional domains are the active part of the protein that is used by the protein for interacting with other proteins or other substances. The job ID for finding the functional domain of 3D23 is www.ebi.ac.uk/interpro/result/InterProScan

Figure 4.2 shows the functional domains of the protein to be targeted. One polypeptide is formed by the combination of two protomers, A and B. There are 1-306 residues in it. There are three domains in each protomer; Domain II

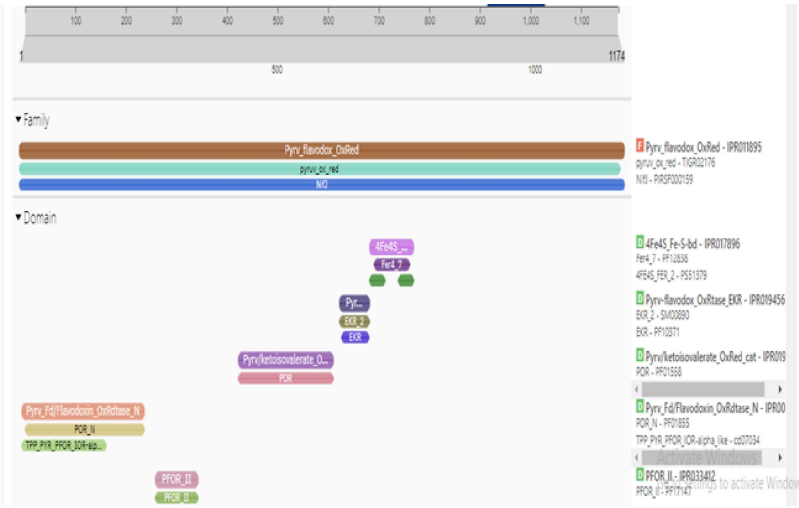

FIGURE 4.2: Functional domains of targeted protein.

has 102-184 residues whereas Domain I has 8-101 residues. The residue count of the third domain is 201-303. A cleft in Domains I and II serves as a location for substrate binding [49].

4.2 Structure of Protein Refined for Docking

The protein structure is refined by the use of PyMol. The extra side-chain C is also removed as shown in Figure 4.3, now the protein is ready for docking. Domains I and II have an antiparallel β-barrel structure whereas Domain III has a globular cluster which consists of five antiparallel α-helices. Domain III is connected by Domain II by a loop region consisting of 185-200 residues [49].

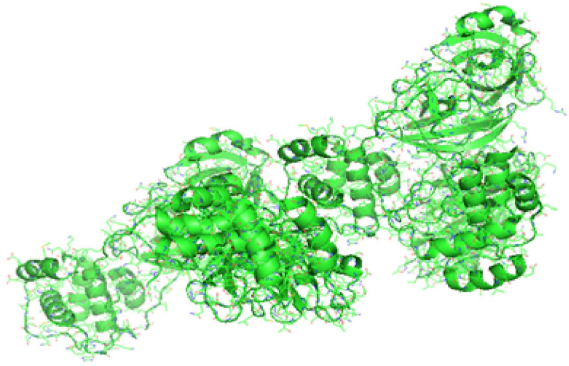

FIGURE 4.3: 3D23 cleaned Protein of M^{pro} of HCoV-HKU1

4.3 Ligand Selection

The selection of ligands is primarily based on several criteria: the best resolution structure, the chemical class of the crystal bound to the protein, and their binding affinities. Conformational selection of the ligand holds significance in this process, wherein a ligand selectively binds to one of the conformers, reinforcing it, and consequently increasing its presence relative to the total protein population [27–30, 51].

To identify potential ligands, a search was conducted within PubChem, recognized as the largest chemical databank globally, to isolate active ingredients from the selected plant. The 3D structures of these ligands were obtained in the SDF format from PubChem and are outlined in Table 4.2, providing structural information [27–30, 51].

Upon acquiring the structures of the selected ligands, the subsequent step involved minimizing the energy of these ligands. This step is critical because using the downloaded structures directly isn't viable due to ligands' instability, which could significantly impact the accuracy of the docking vina scores.

TABLE 4.2: 3D Structure of Selected ligands with molecular formula and molecular structure

S. No	**Ligands Name**	**Molecular Formula**	**Molecular Weight**	**Structure**
1.	Afzelechin	$C_{15}H_{14}0_5$	274.27 g/mol	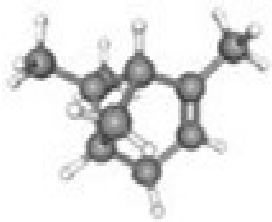
2.	Lupeol	$C_{30}H_{50}O$	426.7 g/mol	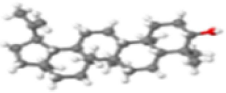
3.	Kaempferol	$C_{15}H_{10}O_6$	286.24 g/mol	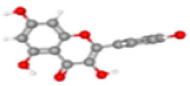

S. No	Ligands Name	Molecular Formula	Molecular Weight	Structure
4.	Catechin	$C_{22}H_{18}O_{10}$	442.37 g/mol	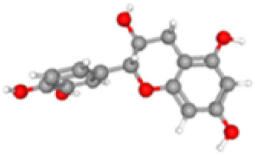
5.	Scoparone	$C_{11}H_{10}O_4$	206.19 g/mol	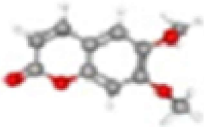
6.	Quercetin	$C_{15}H_{10}O_7$	302.23 g/mol	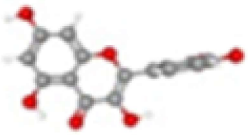
7.	Quinic acid	$C_7H_{12}O_6$	192.17 g/mol	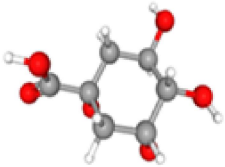
8.	Rutin	$C_{27}H_{30}O_{16}$	610.5 g/mol	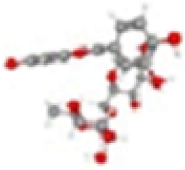
9.	Furosin	$C_{27}H_{22}O_{19}$	650.5 g/mol	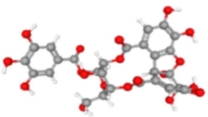
10.	Chrysoplenetin	$C_{19}H_{18}O_8$	374.3 g/mol	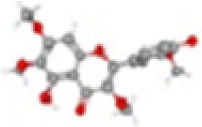
11.	Rhoifolin	$C_{27}H_{30}O_{14}$	578.5 g/mol	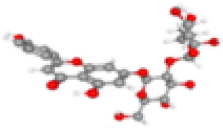
12.	Arteannunin b	$C_{15}H_{20}O_3$	248.32 g/mol	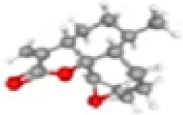

S. No	Ligands Name	Molecular Formula	Molecular Weight	Structure
13.	Oleanolic acid	$C_{30}H_{48}O_3$	456.17 g/mol	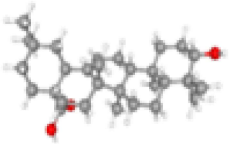
14.	artemisinin	$C_{15}H_{22}O_5$	282.33 g/mol	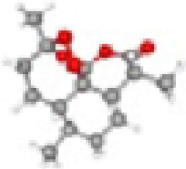
15.	Artemisnic acid	$C_{15}H_{22}O_2$	234.33 g/mol	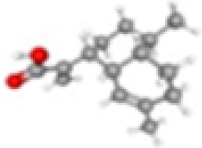
16.	Deoxyartemisnin	$C_{15}H_{22}O_4$	266.33 g/mol	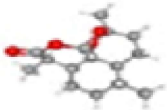
17.	Artemetin	$C_{20}H_{20}O_8$	388.4 g/mol	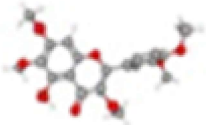
18.	Casticin	$C_{19}H_{18}O_8$	374.3 g/mol	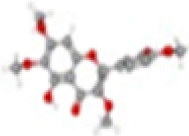
19.	Sitogluside	$C_{35}H_{60}O_6$	576.8 g/mol	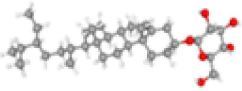
20.	Spinacetin	$C_{17}H_{14}O_8$	346.3 g/mol	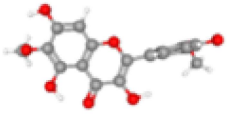
21.	Apigenin	$C_{15}H_{10}O_5$	270.25 g/mol	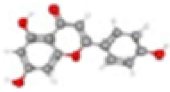

S. No	Ligands Name	Molecular Formula	Molecular Weight	Structure
22.	Kanizol F	$C_{25}H_{28}O_4$	392.5g/mol	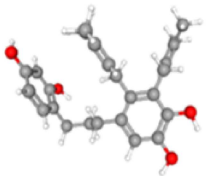
23.	Stigmasterol	$C_{16}H_{26}O$	412.7 g/mol	
24.	Taraxerol	$C_{30}H_{50}O$	426.7g/mol	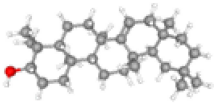
25.	Beta sitosterol	$C_{29}H_{50}O$	414.7 g/mol	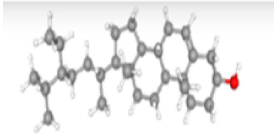

TABLE 4.3: Fifteen selected ligands with structural information

S. No	Ligand	P-value	Molecular Weight	H-Bond Acceptor	H-Bond Donor
1.	Afzelechin	1.8405	274.27 g/mol	5	4
2.	Kaempferol	2.2824	286.2 g/mol	6	4
3.	Catechin	2.5276	150.22 g/mol	10	0
4.	Chrysoplenetin	2.9056	374.34 g/mol	8	2
5.	Arteanniun B	2.4518	248.32 g/mol	3	0
6.	Artemisinic acid	3.645	234.33 g/mol	1	1
7.	Quercetin	1.988	302.23 g/mol	7	5
8.	Rutin	-1.6871	610.5 g/mol	16	10
9.	Deoxyartemisnin	2.4633	266.33 g/mol	4	0
10.	Casiticin	2.9056	374.3 g/mol	8	2
11.	Spinacetin	2.2996	346.29 g/mol	8	4
12.	Artemisinin	2.3949	282.33 g/mol	5	0
13.	Apigenin	2.5768	270.24 g/mol	5	3
14.	Scoparone	1.8102	206.19 g/mol	4	0
15.	Kanizol F	5.707	396.5 g/mol	4	4

In Table 4.3 we have selected fifteen Ligands, rutin does not follow the Lipinski rule at all while all other ligands obeys the Lipinski rule.

4.3.1 Toxicity Prediction

The values of ADMET (Absorption, Distribution, Metabolism, Excretion, and Toxicity) for bioactive substances and medications may be predicted using the web program PkCSM. By using this tool, we had determined the toxicity of the ligands selected, for these different methods are used to test whether a given ligand is toxic or not. The AMES toxicity test uses microbes to assess a compound's potential for mutagenicity. If it shows a positive response, then the ligand is mutagenic which can also act as a carcinogen *T. Pyriformis* toxicity method uses *T. Pyriformis* (protozoa bacteria) toxicity as a toxic endpoint. Any value >-0.5 log ug/L is considered toxic. The values predicted in the Minnow toxicity test are used to represent the concentration at which the compound could cause the death of 50% of the minnows. The value below 0.5 mM is regarded as acute toxic. The values for MRTD (maximum recommended tolerated dose) give a picture of the starting dose of a certain pharmaceutical at clinical phase I. Value $\geq$ 0.477 log mg/kg/day is low and a value greater than this value is considered as high. For the oral rat chronic test of toxicity, the predicted log value of the lowest observed adverse effect in log mg/kg/day is given which relates to the concentration of the compound given that requires the treatment time. A hepatotoxicity test predicts that if a compound could affect the liver functioning or not. A skin test predicts whether the compound could give any skin reactions or not [52–54].

The hERG I and II inhibitor test determine the potential of any compound to cause the inhibition of the potassium channels associated with hERG. An inhibitor of these channels could lead to QT syndrome and on a long-term basis the person could develop ventricular arrhythmia [52–54]. The toxicity predicted values of the selected ligands are shown in the Tables from 4.4 to 4.10.

4.3.1.1 Determination of Toxicity Values of Afzelechin, Kaempferol, Catechin and Chrysoplenetin

The toxicity values of afzelechin, kaempferol catechin and chrysoplenetin are given below. Table 4.4 shows that kaempferol and chrysoplenetin has a high MRTD

value. All other test values are in the safe range, that shows that both afzelechin and kaempferol are not the cause for AMES toxicity, afzelechin have a safe tolerated dose. It also shows that all are not hERG I and II inhibitors except only catechin is inhibitors to hERG II. All have a safe toxic rate with respect to test on rat and on *T. pyriformis* with that they are not toxic to liver and does not provide any sensitivity to skin [52–54].

TABLE 4.4: Toxicity values of afzelechin and kaempferol, catechin and chrysoplenetin

S. No	**Model Name**	**Predicted values of Afzelechin**	**Predicted values of Kaempferol**	**Predicted values of Catechin**	**Predicted values of Chrysoplenetin**
1.	AMES Toxicity	No	No	No	No
2.	Max. tolerated dose (human)	0.136	0.531	0.449	0.491
3.	hERG I inhibitor	No	No	No	No
4.	hERG II inhibitor	No	No	Yes	No
5.	Oral rate acute toxicity	2.365	2.449	2.558	2.324
6.	Oral rate Chronic toxicity	2.215	2.505	2.777	1.773
7.	Hepatoxicity	No	No	No	No
8.	Skin sensitization	No	No	No	No
9.	t.pyrisformis toxicity	0.519	0.312	0.285	0.313
10.	Minnow toxicity	2.75	2.885	6.146	2.2248

4.3.1.2 Toxicity Values Determination of ArteanniunB, Artemisinic Acid, Rutin and Quercetin

The toxicity values of arteanniun B, artemisinic acid, rutin and quercetin are given below. Table 4.5 shows that arteanniun B, artemisinic acid has a low and rutin and quercetin have high MRTD value. All other test values are in the safe range. It also shows that all are not hERG I and II inhibitors except only rutin can inhibit to hERG II. All have a safe toxic rate with respect to test on rat and

on *T. pyriformis* with that they are not toxic to liver and does not provide any sensitivity to skin [54, 55].

TABLE 4.5: Toxicity Values of Arteanniun B , Artemisinic Acid, Rutin and Quercetin

S. No	**Model Name**	**Predicted values of Arteanniun B**	**Predicted values of artemisinic acid**	**Predicted values of rutin**	**Predicted values of quercetin**
1.	AMES Toxicity	No	No	No	No
2.	Max. tolerated dose (human)	0.195	0.403	0.452	0.47
3.	hERG I inhibitor	No	No	No	No
4.	hERG II inhibitor	No	No	Yes	No
5.	Oral rate acute toxicity	2.052	1.747	2.491	2.302
6.	Oral rate Chronic toxicity	1.589	2.251	3.673	1.768
7.	Hepatoxicity	No	No	No	No
8.	Skin sensitization	No	Yes	No	No
9.	*T. pyrisformis* toxicity	0.45	0.514	0.285	0.317
10.	Minnow toxicity	1.53	0.541	7.677	2.233

4.3.1.3 Toxicity Values Determination of Deoxyartemisnin, Artemisin -in, Casiticin & Spinacetin

The toxicity values of deoxyartemisnin, artemisinin ,casiticin and spinacetin are given below. Table 4.6 shows that artemisinin is AMES toxic while other have safe range. Deoxyartemisnin and artemisinin has a low MRTD value. All other test values are in the safe range. It also shows that all are not hERG I and II inhibitors . All have a safe toxic rate with respect to test on rat and on *T. pyriformis* with that they are not toxic to liver and does not provide any sensitivity to skin [55].

TABLE 4.6: Toxicity values of Deoxyartemisnin, Casiticin, Artemisinin and Spinacetin

S. No	Model Name	Predicted values of Deoxyartemisnin	Predicted values of Casiticin	Predicted values of Artemisinin	Predicted values of Spinacetin
1.	AMES Toxicity	No	No	Yes	No
2.	Max. tolerated dose (human)	0.174	0.47	0.065	0.652
3.	hERG I inhibitor	No	No	No	No
4.	hERG II inhibitor	No	No	No	No
5.	Oral rate acute toxicity	2.161	2.302	2.459	2.412
6.	Oral rate Chronic toxicity	1.506	1.768	1	2.761
7.	Hepatoxicity	No	No	No	No
8.	Skin sensitization	No	Yes	No	No
9.	t.pyrisformis toxicity	0.363	0.317	0.322	0.293
10.	Minnow toxicity	1.538	2.233	1.406	2.151

4.3.1.4 Determination of Toxicity Values of Apigenin, Scoparone and Kanizol f.

The toxicity values of apigenin, scoparone, kanizol F are given below in Table 4.7. All the three ligands have shown values in the range that is determined by pkcsm. All of these are not toxic neither are they the inhibitors nor does any harm to skin and to the liver [54].

TABLE 4.7: Toxicity values of Apigenin, Scoparone and Kanizol f

S. No	Model Name	Predicted values of Apigenin	Predicted values of Scoparone	Predicted values of Kanizol f
1.	AMES Toxicity	No	No	No
2.	Max. tolerated dose (human)	0.328	0.494	0.501

TABLE 4.7: Toxicity values of Apigenin, Scoparone and Kanizol f

S. No	Model Name	Predicted values of Apigenin	Predicted values of Scoparone	Predicted values of Kanizol f
3.	hERG I inhibitor	No	No	No
4.	hERG II inhibitor	No	No	No
5.	Oral rate acute toxicity	2.45	2.345	2.215
6.	Oral rate Chronic toxicity	2.298	2.048	1.298
7.	Hepatoxicity	No	No	No
8.	Skin sensitization	No	No	No
9.	t.pyrisformis toxicity	0.38	0.603	0.296
10.	Minnow toxicity	2.232	1.223	0.728

The toxicity values mentioned in the above Tables from 4.4 to 4.7 shows that based on toxicity tests like skin sensation, hERG II inhibitors, AMES toxicity, and minnow toxicity we would screen out artemisinin, casiticin, rutin, artemisinic acid, catechin, dihydroartemisinic, all other ligands pass the toxicity test, but the final screening would be based on the overall ADME properties.

4.4 Molecular Docking

Molecular docking is an approach that determines the proper structure of the ligand that binds to the binding site and estimates the strength between a ligand attached to a receptor protein using the vina score function. The 3D structure of the ligands and the protein are taken to perform docking. For this purpose, CB dock an online blind auto docking tool is used [52, 54].

CB Dock computes the cavity sizes and predicts the protein binding locations. CB Dock provides us with the top five possess and receptor models upon docking. Based on the cavity size and the vina score, the optimal position was chosen among these five [53, 54].

Molecular docking was performed by using M^{pro} as the receptor protein and the fifteen ligands selected above. The protein was in the PDB format and the ligands were in the SDF format. CB dock then checked the input files and then converted them into pdbqt format files by using OpenBabel and MGL Tools [54]. Then CB dock predicted the cavities of the receptor and also calculated the centers and sizes of the top five cavities. Among the five best conformations the best one was selected based on a high-affinity score of the interaction between the protein and the ligand [54]. Ligands showing the best binding score between the selected ligands and the protein M^{pro} are shown in Tables 4.11-4.18.

Table 4.8 shows the docking result of all selected ligands. It shows that afzelechin has binding score of -7.5. The logP value of this docked result is 1.8405. kaemferol shows the docking score of -7.9, and gives a logP value of 2.282. Afzelechin and kaempferol have shown a low binding score than that of catechin. Catechin shows a binding score of -8 and log p value is 1.5461.Rutin is also showing the highest binding score of -8.9 while , chrysoplenetin also shows a binding score of -7.9 and arteanniun B shows a score of -6.8. Artemisinic acid shows the same binding score of -7.2. Quercetin shows a score of -8.5, and deoxyartemisnin shows score of -7.3. Casiticin shows the binding score of -7.5 and both apigenin and spinacetin shows the score of -7.8. Scoparone and kanizol f and artemisinin shows a binding score of -6.1 and -7.7 and -7.7 respectively.

Table 4.8: Docking result of all selected Ligands

S No	**Ligands**	**Binding Score**	**Cavity size**	**HBD**	**HBA**	**Log P**	**M. Weight**	**Rotatble Bond**	**Grid Map**
1.	Afzelechin	-7.5	1309	4	5	1.8405	274.2	1	53.075
2.	Kaempferol	-7.9	1309	4	6	2.282	286.23	1	53.075
3.	Catechin	-8	1309	5	6	1.5461	290.2	1	53.057
4.	Chryso plenetin	-7.9	1309	2	8	2.9056	374.35	5	-53
5.	Arteanniun B	-6.8	3488	0	3	2.451	248.32	0	-49
6.	Rutin	-9.7	3488	10	16	-1.678	610.5	6	-49
7.	Quercetin	-8.5	1309	5	7	1.988	302.23	1	-53

TABLE 4.8: Docking result of all selected Ligands

S No	Ligands	Binding Score	Cavity size	HBD	HBA	Log P	M. Weight	Rotatble Bond	Grid Map
8.	Artemisinic acid	-7.2	753	1	1	-3.645	243.3	2	-56
9.	Deoxy artemisnin	-7.3	3448	0	4	2.4633	266.33	0	-49
10.	Casiticin	-7.5	3448	2	8	2.9056	374.34	5	-49
11.	Spinacetin	-7.8	3448	4	8	2.2996	346.3	3	-49
12.	Artemisinin	-7.7	753	0	5	2.3949	282.336	0	-56
13.	Apigenin	-7.8	1309	3	5	2.5678	270.2	1	-53
14.	Scoparone	-6.1	3448	0	4	1.8102	206.197	2	-47
15.	Kanizol F	-7.7	3448	4	4	5.7017	396.5	8	-49

Ligands like afzelechin, kaempferol and Catechin had already been reported to be docked against the M^{pro} by using Auto dock. Afzelechin shows the same binding score of -7.5 as already been reported by P Bhattacharya, TN Patel – 2021 kaempferol show a score of -7.9 and catechin show s binding score of -8 [52].

Ligands like quercetin, rutin and apigenin had already been reported to be docked against the M^{pro} by using Auto dock wizard. Quercetin shows the binding score of -7.2 which is lesser than the docking score showed by CB-Dock as already been reported by Oluwaseun Taofeek in 2020 [55]. Ligands like chrysoplenetin, arteanniun B and rutin had already been reported to be docked against the M^{pro} by using Auto dock wizard. chrysoplenetin shows the binding score of -7.9 which is lesser than the docking score showed by CB-Dock as already been reported by Oluwaseun Taofeek in 2020 [55].

4.5 Ligands' Interaction with the Targeted Protein

PyMol and LigPlot are employed for analyzing the docking result. LigPlot is employed to predict an association between the ligands and the protein that serves as

the receptor. LigPlot's graphical system utilizes the 3D coordinates to generate on its own two-dimensional representations of interactions. The two-dimensional images illustrate the hydrophobic and hydrogen bond interactions that occur between the ligand and side chain or main chain elements of the receptor protein [54]. The 2D diagrams of the interaction of the ligands and the protein are shown in figures 4.4 - 4.18 whereas table 4.9 shows the hydrogen and hydrophobic interactions.

Figure 4.4 shows the bonding interaction of afzelechin with receptor protein M^{pro}. It shows that afzelechin has formed nine hydrophobic interactions and four hydrogen Bonds.

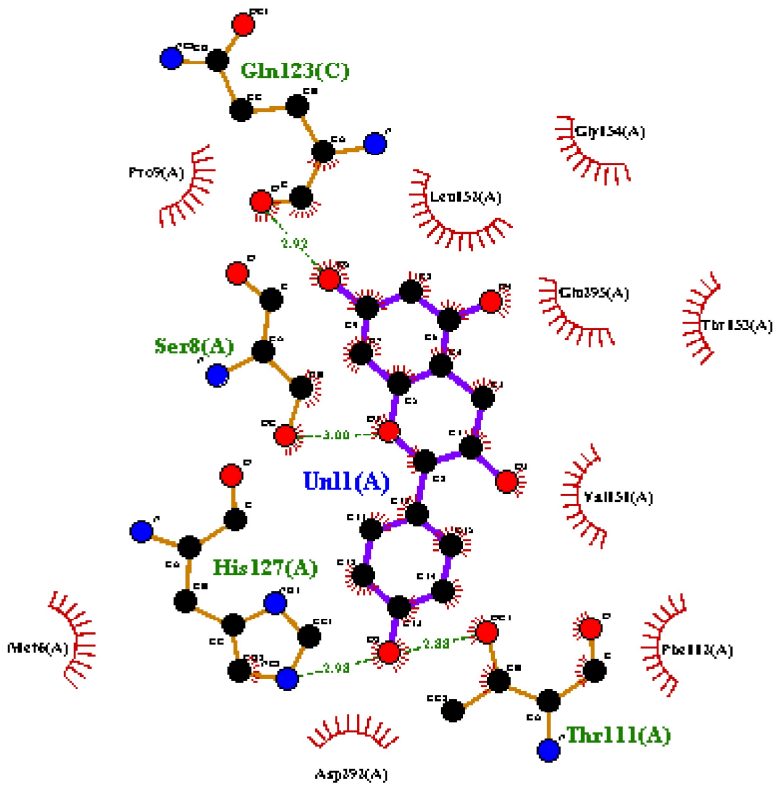

FIGURE 4.4: Interaction of afzelechin with the receptor protein

Figure 4.5 shows the interaction of kaempferol with receptor protein M^{pro}. It shows that kaempferol has formed nine hydrophobic interactions and four hydrogen bond.

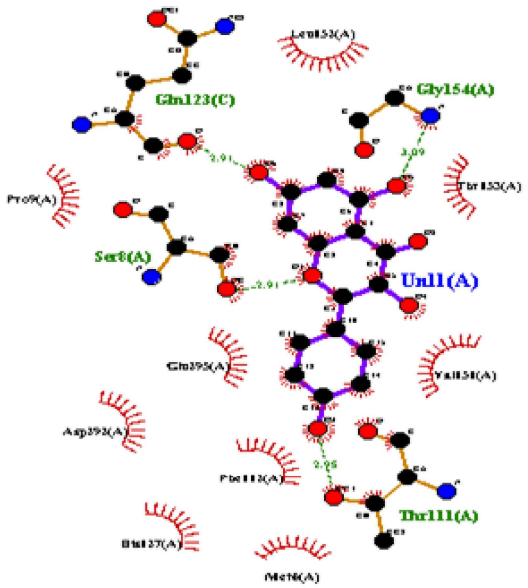

FIGURE 4.5: Interaction of kaempferol with receptor protein

Figure 4.6 shows the interaction of catechin with receptor protein M^{pro}. It shows that catechin has formed seven hydrophobic interactions and six hydrogen bond.

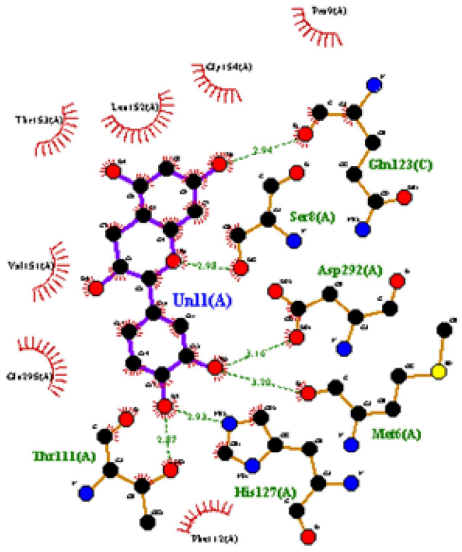

FIGURE 4.6: Interaction of catechin with receptor protein

Figure 4.7 shows the interaction of chrysoplenetin with receptor protein M^{pro}. It shows that chrysoplenetin has formed nine hydrophobic interactions and five hydrogen bonds

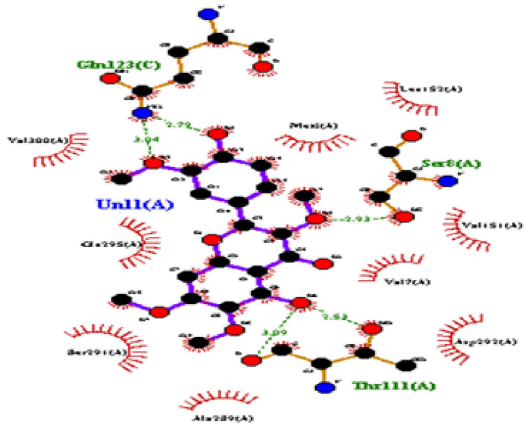

FIGURE 4.7: Interaction of chrysoplenetin with receptor protein

Figure 4.8 shows the interaction of arteanniun B with receptor protein M^{pro}. It shows that Arteanniun B has formed nine hydrophobic interactions and five hydrogen bonds.

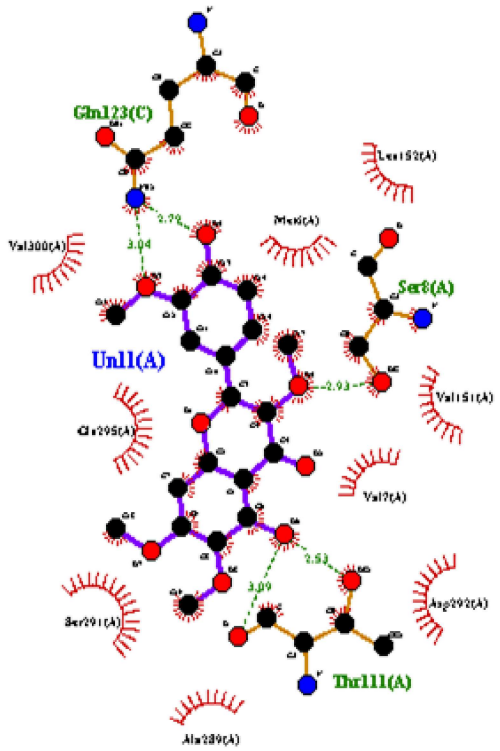

FIGURE 4.8: Interaction of arteanniun B with receptor protein

Figure 4.9 shows the interaction of rutin with receptor protein M^{pro}. It shows that rutin has formed fourteen hydrophobic interactions and seven hydrogen bonds.

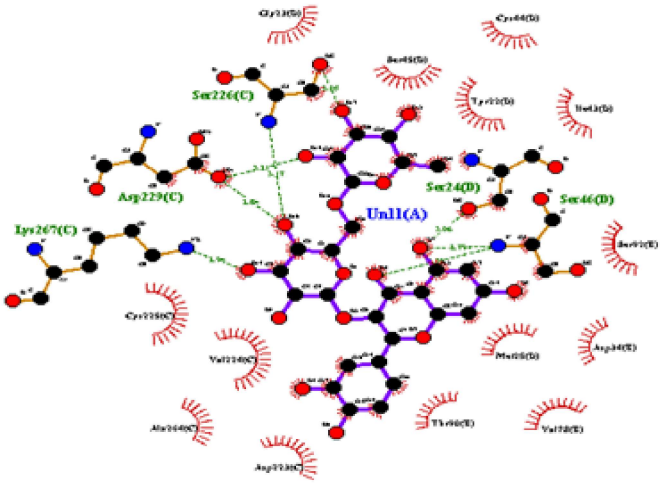

FIGURE 4.9: Interaction of rutin with receptor protein

Figure 4.10 shows the interaction of quercetin with receptor protein M^{pro}. It shows that quercetin has formed seven hydrophobic interactions and six hydrogen bonds.

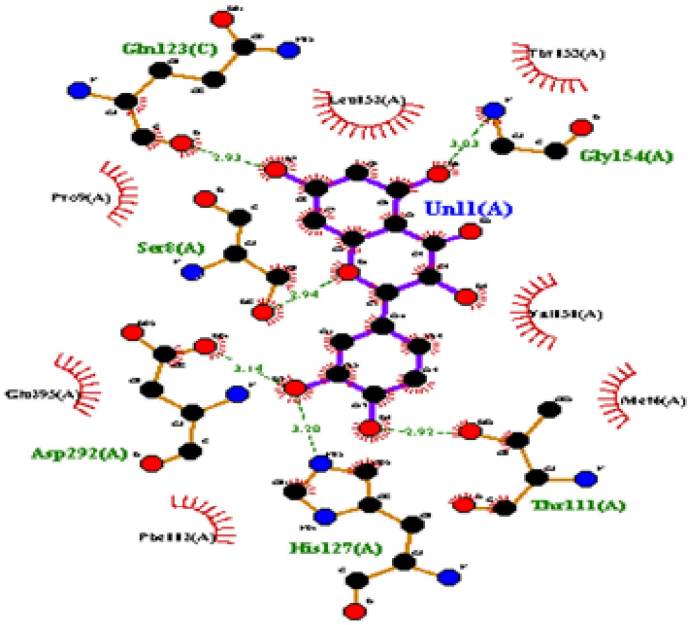

FIGURE 4.10: Interaction of quercetin with receptor protein

Figure 4.11 shows the interaction of artemisinic acid with receptor protein M^{pro}. It shows that artemisinic acid has formed seven hydrophobic interactions and three hydrogen bonds.

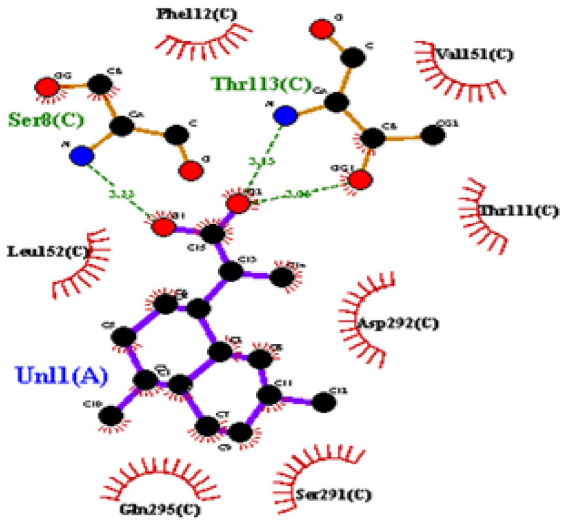

FIGURE 4.11: Interaction of artemisinic acid with receptor protein

Figure 4.12 shows the interaction of deoxyartemisnin with receptor protein M^{pro}. It shows that deoxyartemisnin has formed ten hydrophobic interactions and two hydrogen bonds.

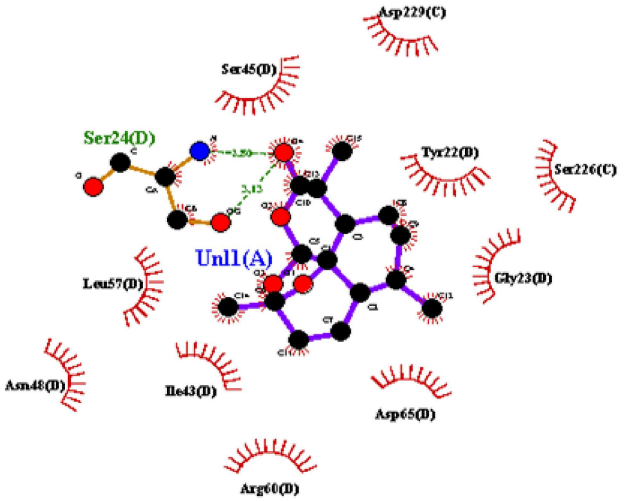

FIGURE 4.12: Interaction of deoxyartemisnin with receptor protein

Figure 4.13 shows the interaction of casiticin with receptor protein M^{pro}. It shows that casiticin has formed twelve hydrophobic interactions and two hydrogen bonds.

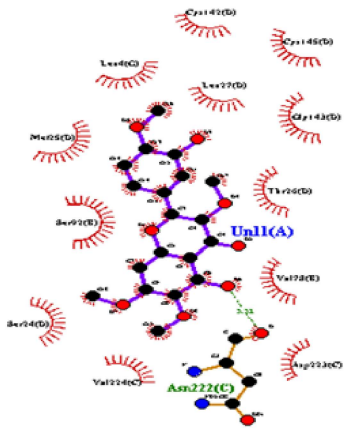

FIGURE 4.13: Interaction of casiticin with receptor protein

Figure 4.14 shows the interaction of spinacetin with receptor protein M^{pro}. It shows that spinacetin has formed thirteen hydrophobic interactions and two hydrogen bonds.

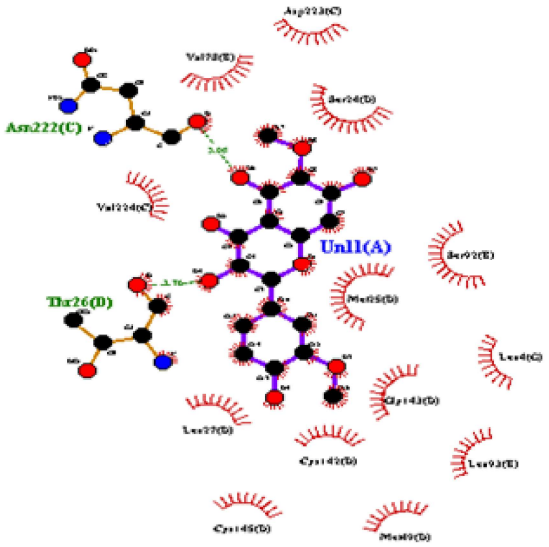

FIGURE 4.14: Interaction of spinacetin with receptor protein

Figure 4.15 shows the interaction of apigenin with receptor protein M^{pro}. It shows that apigenin has formed ten hydrophobic interactions and four hydro gen bonds.

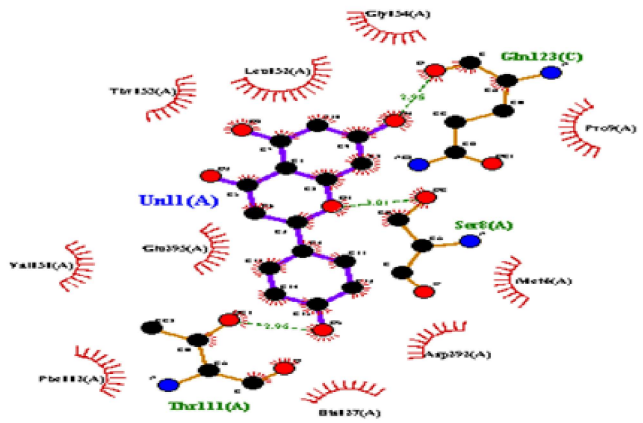

FIGURE 4.15: Interaction of apigenin with receptor protein

Figure 4.16 shows the interaction of scoparone with receptor protein M^{pro}. It shows that scoparone has formed six hydrophobic interactions and five hydrogen bonds.

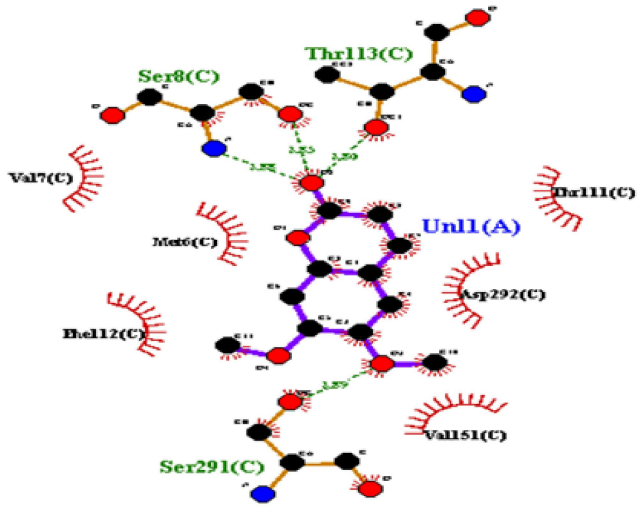

FIGURE 4.16: Interaction of scoparone with receptor protein

Figure 4.17 shows the interaction of artemisinin at cavity with receptor protein M^{pro}. It shows that artemisinin has formed twelve hydrophobic interactions.

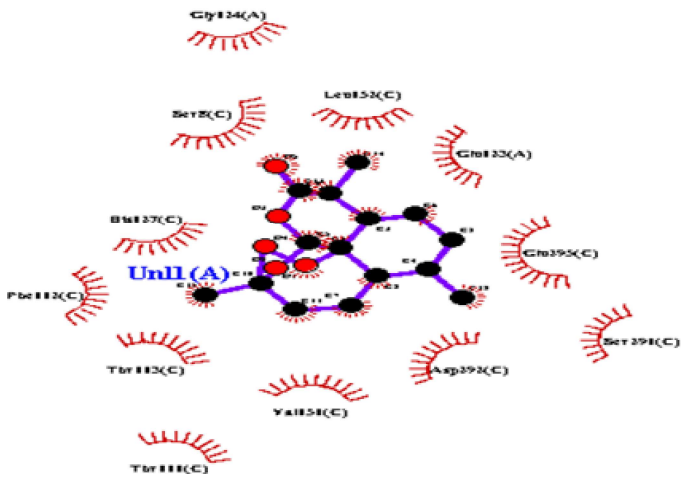

FIGURE 4.17: Interaction of artemisinin with receptor protein

Figure 4.18 shows the interaction of kanizol F with receptor protein M^{pro}. It shows that kanizol F has formed twelve hydrophobic interactions and four hydrogen bonds.

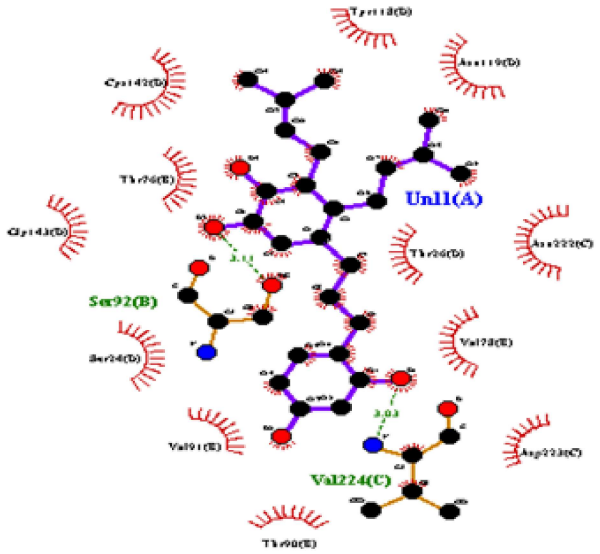

FIGURE 4.18: Interaction of kanizol F with receptor protein

The Table 4.9 below shows the details of hydrogen and hydrophobic interactions of the selected ligands with the receptor protein. The values show that rutin forms the highest hydrophobic interactions in number which is fourteen next

spinacetin is thirteen hydrophobic interactions whereas casiticin, kanizol f, and artemisinin with 12 hydrophobic bonds, ten hydrophobic bonds are made by apigenin and deoxyartemisnin, while afzelechin, kaempferol, artemisinic acid, arteanniun, and chrysoplenetin with those 9 hydrophobic interactions while catechin, quercetin artemisinic acid form seven hydrophobic interactions. The hydrogen bonds formed by rutin is 7 which is the highest in number out of all the selected ligands whereas quercetin, catechin forms six hydrogen bonds. Arteanniun B, scoparone and chrysoplenetin forms five hydrogen bonds.

Table 4.9: Active ligand showing hydrogen and Hydrophobic Interactions

S. No	**Ligand Name**	**Binding Energy**	**No of HB**	**Bonding Amino Acids**	**Distance**	**Hydrophobic Bonding**
1.	Afzelechin	-7.5	4	N-Ser8-O	2.92	Gly154 Thr153
				N-Gln123-O	3.00	Val151 Phe112
				O-His127-C	2.88	Asp292 Met6
				OG1-His127-O	2.98	Pro9 Leu152
						Gln295
2.	Kaempferol	-7.9	4	N-Gly154-O	2.95	His127 Thr153
				N-Ser8-O	2.91	Val151 Phe112
				O-Gln123-N	3.09	Asp292 Met6
				N-Thr111-O	2.91	Pro9 Leu152
						Gln295
3.	Catechin	-8	5	O-Gln123-O6	2.37	Pro9A Gly154
				N-Asp292-O	3.16	Leu152 Thr153
				N-Met6-O	3.20	Val151 Gln295
				N-His127-O	2.93	Phe112
				O-Thr111-OG1	2.94	
4.	Chrysoplenetin	-7.9	5	OG1-Thr111-O6	2.53	Leu152 Met6
				O-Thr111-O6	3.09	Val151 Val7
				N-Gln123-O	2.93	Asp292 Ala289
				O-Gln123-N	3.04	Ser291 Gln295
				OG-Ser8-N	2.79	Val300
5.	Arteanniun B	-6.8	0	-	-	Asp65 Gly23
						Ser226 Tyr22
						Leu57 Arg60
						Glu228

TABLE 4.9: Active ligand showing hydrogen and Hydrophobic Interactions

S. No	Ligand Name	Binding Energy	No of HB	Bonding Amino Acids	Distance	Hydrophobic Bonding
6.	Rutin	-9.7	7	O-Ser46-N	3.30	Ala264 Val224
				N-Ser46-O	3.17	Cys225 Asp223
				N-Lys267-O	3.31	Thr90 Val78
				N-Asp229-OP1	3.05	Met25 Asp34
				O-OP1-O16	2.54	Ser92 Ile43
				N-Ser226-O	2.79	Tyr22 Ser45
				O-Gly123-N	2.94	Gly23 Cys44
7.	Artemisinic Acid	-7.2	3	OG1-Thr113-O2	3.06	Leu57 Arg60
				N-Thr113-O3	3.22	Cys44 Ile43
				N-Ser8-O	3.15	Tyr22 Asp65
						Gly23 Ser226
						Glu228
8.	Quercetin	-8.5	6	N-Gly154-O	3.03	Thr153 Leu152
				O-Gln123-OT	2.92	Val151 Met6
				OG1-Ser8-O1	2.94	Phe112 Gln295
				N-Thr111-O	3.14	Pro9
				N-His127-O2	3.20	
				OG1-Asp292-O3	2.93	
9.	Deoxyartemisnin	-7.3	2	N-Ser24-O4	3.13	Ser45 Asp229
				O-Ser24-OG	2.80	Tyr22 Ser226
						Gly23 Leu57
						Asn48 Ile43
						Arg60 Asp65
10.	Casiticin	-7.5	1	O-Asn222-C3	3.32	Leu 4 Met25
						Ser92 Cys142
						Leu27 Gly143
						Cys145 Val178
						Asp223 Ser24
						Val224 Thr26
11.	Spinacetin	-7.8	2	O-Asn222-O6	3.76	Asp223 Val78
				O-Thr26-O5	3.05	Ser24 Met25
						Cys142 Leu27
						Ser92 Gly143

Table 4.9: Active ligand showing hydrogen and Hydrophobic Interactions

S. No	Ligand Name	Binding Energy	No of HB	Bonding Amino Acids	Distance	Hydrophobic Bonding
						Leu4 Leu93 Met49 Cyst145 Val224
12.	Apigenin	-7.8	3	O-Gln123-ON OG-Ser8-O1 OG1-Thr111-O5	2.95 3.01 2.96	Gly154 Leu152 Thr153 Pro9 Met6 Asp292 His127 Phe112 Val151 Gln295
13.	Artemisinin	-7.7	1	OG-Ser70-O4	2.99	Thr111 Thr113 Phe112 His127 Ser8 Gly124 Leu152 Gln123 Gln295 Ser291 Val151 Asp292
14.	Scoparone	-6.1	3	O2-Ser45-OG O2-Ser45-N O2-Asn48-N	3.14 3.01 3.12	Asp65 Glu228 Arg60 Leu57 Cys44 Ile43 Gly23 Tyr22 Asp65
15.	Kanizol F	-7.7	2	O-Ser92-O2 N-Val224-O1	3.03 3.11	Thr90Val91 Ser24Gly143 Thr76Cys142 Tyr118Asn119 Thr26Asn222 Val78Asp223

4.6 ADMET Properties

In order to determine if something is vocally or artificially available, Lipinski's Five Drug Laws are first applied [46]. pkCSM is the second tool that is used for the assessment of ADMET properties [45].

4.6.1 Pharmacodynamics

One of the broader terms used in pharmacology is pharmacodynamics which is concerned with researching how drugs affect the body [54].

4.6.2 Pharmacokinetics

The other term used in pharmacology is pharmacokinetics which deals with the study of the reaction of the body to the drug, that how the body reacts after the drug enters the body. The absorption, distribution, metabolism, and excretion of drugs are also studied [54].

4.6.3 Absorption

The $CaCO_2$ solubility helps in predicting the absorption of the drugs which are administered orally. Value > 0.90 (log Papp in 10-6 cm/s) is considered as high $CaCO_2$ permeability [52, 53].The water solubility of the ligands is given as log mol/L. this indicates the compound solubility in water at 25°C. hence the lipid-soluble drugs will be less soluble than the water-soluble drugs. Intestinal absorption indicates the value or proportion of the compound that will absorb into the intestines. A value less than 30% is considered poorly absorbed [53–56].

P-glycoprotein is an ABC transporter that functions to extrude toxins or other xenobiotics from the cells by acting as a biological barrier. p-glycoprotein inhibition can be a therapeutic target or it can act in contradiction. Skin permeability is important for developing transdermal drugs.Any compound with a value > -2.5 has a low skin permeability [53–56].

The absorption properties of all selected ligands are given in the Table 4.10. It shows that afzelechin, kaempferol, catechin, chrysoplenetin all have low skin permeability and also has low $CaCO_2$ solubility. Apart from all these the values of other parameters are in the range, chrysoplenetin is not the inhibitors of P

-glycoprotein II. It also reports that quercetin, and rutin have low $CaCO_2$ solubility. With that rutin also have low intestinal absorption. Whereas rutin and quercetin are p glycoprotein substrate. While deoxyartemisnin and artemisinin are not P-glycoprotein substrates, with that casiticin also has low skin permeability. Other than that Water solubility, $CaCO_2$ solubility, intestinal absorption values are all in the pkcsm range. Deoxyartemisnin,rutin and artemisinin are not the P-glycoprotein I and II Except casiticin which is inhibitors of P-glycoprotein II. kanizol F has low $CaCO_2$ solubility with that it also is a P-glycoprotein II inhibitor only. Whereas scoparone is not a P-glycoprotein substrate and also is not inhibitor of P-glycoprotein I and II. Apigenin gives the values of absorption parameters which are water solubility, $CaCO_2$ solubility, intestinal absorption, skin permeability, P-glycoprotein substrate and its inhibitors, all have indicated the values in pkcsm range.

Table 4.10: Absorption properties of all selected ligands

S No	Ligands	Water Solubility	$CaCO_2$ Solubility	Intestinal Absorption (human)	Skin Permeability	P glycoprotein Substrate	P glycoprotein I Inhibitor	P glycoprotein II Inhibitor
1.	Afzelechin	-3.254	1.077	91.482	-2.735	yes	No	No
2.	Kaempferol	3.04	0.032	74.29	-2.735	Yes	No	No
3.	Catechin	-3.117	-0.283	68.829	-2.735	Yes	No	No
4.	Chrysoplenetin	-3.605	1.393	99.856	-2.743	Yes	No	Yes
5.	Arteanniun B	-3.221	1.537	98.347	-3.322	No	No	No
6.	Artemisinic acid	-3.632	1.6	95.706	-2.699	No	No	No
7.	Quercetin	-2.925	-0.229	77.207	-2.735	Yes	No	No
8.	Rutin	-2.892	-0.949	23.446	-2.735	Yes	No	No
9.	Deoxy artemisnin	-3.396	1.318	97.828	-3.279	No	No	No
10.	Casiticin	-3.599	1.39	96.91	-2.744	Yes	No	Yes
11.	Spinacetin	-3.126	-0.158	67.925	-2.735	Yes	No	No
12.	Artemisinin	-3.448	1.279	97.785	-3.314	No	No	No
13.	Apigenin	-3.329	1.007	93.25	-2.735	Yes	No	No
14.	Scoparone	-1.976	1.298	97.879	-2.346	No	No	No
15.	Kanizol F	-3.443	0.844	89.18	-2.735	Yes	Yes	Yes

Some of the parameters of absorption properties of afzelechin has already been studied by P Bhattacharya, TN Patel – 2021 [52]. Some parameters of absorption properties of kaempferol and catechin have been studied by Erman Salih in

2020 [53]. Pkcsm absorption properties of chrysoplenetin, casiticin, artemisinin, spinacetin and deoxyartemisnin has already been reported by Zarina Khurshid in 2021 [54]. Pkcsm absorption properties of apigenin have already been reported by Zarina Khurshid in 2021 [54]. Some parameters of absorption of quercetin, rutin and apigenin have been studied by Oluwaseun Taofeek in 2020 [55]. Absorption properties of Scoparone and Kanizol f has already been reported by Muthu Manickam Sankar and his colleagues in 2021 [57].

4.6.4 Distribution

The VDss is the estimated volume which tells about the entire dose of the drug which will be needed to be distributed uniformly to give the same concentration as it is in the blood plasma. If the VDss value exceeds 2.81 L/kg, then the drug is more dispersed throughout the tissues compared to the plasma. The VDss will be low if the value is below 0.71 L/kg [54].

Many drugs in the plasma exist in an equilibrium between a bounded and an unbounded state to the serum proteins. As a drug binds more to the serum proteins it will have less efficiency of diffusion to cellular membranes. The blood-brain barrier protects the brain and reduces the exogenous compounds to enter directly into the brain. If a compound has a value of logBB >0.3 then it will easily cross the BBB barrier hence been effective and if it is logBB < -1 then it is poorly distributed [54]. Compounds with a value of logPS>-2 penetrate the CNS whereas value logPS <-3 does not penetrate the CNS [54].

The values of the distribution of all selected ligands are given below in Table 4.11. The parameters through which the distribution properties are determined includes VDss which is in the given in table that afzelechin, kaempferol, catechin is high while in chrysoplenetin value is low, the all ligands have low BBB values so they are poorly distributed to brain. The values of the fraction unbound of these ligands shows that out of the total dose this fraction will not be bounded to the protein. All these ligands mentioned in table 4.18 cannot cross the blood brain barriers whereas catechin and chrysoplenetin out of all these will not pass the CNS. It also

indicates that quercetin and rutin cannot cross the blood brain barrier and with that both are also not permeable to central nervous system. Other parameters give the distribution of ligands and gives the amount of the unbounded ligand. The table also show the value which indicates that deoxyartemisnin, artemisinin is permeable to the central nervous system except spinacetin, casiticin it also shows that these ligands cannot easily cross the blood brain barrier. While apigenin, scoparone and kanizol f all three ligands as drugs can pass through the central nervous system and cannot penetrate through blood brain barrier.

TABLE 4.11: Distribution of properties of all selected ligands

S No	**Ligands**	**VDss (Human)**	**Fraction Unbound (Human)**	**BBB Permeability**	**CNS Permeability**
1.	Afzelechin	0.562	0.194	-0.818	-2.473
2.	Kaempferol	1.274	0.178	-0.939	-2.228
3.	Catechin	1.027	0.235	-1.054	-3.298
4.	Chrysoplenetin	-0.161	0.103	-1.043	-3.226
5.	Arteanniun B	0.401	0.426	0.434	-2.951
6.	Artemisinic acid	-0.449	0.302	0.323	-2.314
7.	Quercetin	1.559	0.206	-1.098	-3.065
8.	Rutin	1.663	0.187	-1.899	-5.178
9.	Deoxyartemisnin	0.356	0.411	0.28	-2.999
10.	Casiticin	-0.176	0.103	-1.503	-3.209
11.	Spinacetin	0.675	0.057	1.465	0.235
12.	Artemisinin	0.459	0.445	0.235	-2.933
13.	Apigenin	0.822	0.147	-0.734	-2.061
14.	Scoparone	-0.344	0.298	0.177	-2.328
15.	Kanizol F	-0.028	0.063	-1.001	-2.081

Some of the parameters of distribution properties of afzelechin has already been studied by P Bhattacharya, TN Patel – 2021 [52]. Some parameters of distribution properties of catechin and kaempferol have been studied by Erman Salih I˙STI˙FLI˙ in 2020 [53]. Pkcsm distribution properties of chrysoplenetin, Spinacetin, artemisinin and casiticin has already been reported by Zarina Khurshid in 2021 [54]. Pkcsm Distribution properties of some parameters of distribution of quercetin, rutin and apigenin have been studied by Oluwaseun Taofeek in 2020

[55]. Distribution properties of kanizol f has already been reported by Muthu Manickam Sankar and his colleagues in 2021 [57].

4.6.5 Metabolism

Cytochrome P450 is an enzyme held responsible for detoxification in the liver. Many drugs get deactivated by this enzyme but certain drugs can be activated. Inhibitors of this enzyme can directly affect the metabolism of drug hence should not be used [54–57]. Similarly, CYP2D6 and CYP3A4 are responsible for the metabolism of the drugs. Inhibition to these affects the pharmacokinetics of the drug in use [54–57].

Table 4.12 shows the metabolic properties of all selected ligands. First five ligands that afzelechin, kaempferol, catechin, chrysoplenetin, arteanniun B are neither the CYP2D6 substrate and CYP3A4 substrate, are also not inhibitors to CYP2C9 and CYP2D6 and CYP3A4 and CYP2C19 inhibitors except chrysoplenetin. It indicates that arteanniun B, quercetin, are not CYP2D6, CYP3A4 substrates. While rutin and artemisinic acid are not CYP1A2 inhibitors except Arteanniun B and Quercetin. Also, artemisinic acid, arteanniun B, quercetin, rutin are not CYP2C19, CYP2D6, CYP3A4 and CYP2D6 inhibitors. While deoxyartemisnin, casiticin, are not CYP2D6 substrates. casiticin, artemisinin and deoxyartemisnin are CYP3A4 substrates. Also, deoxyartemisnin, spinacetin are inhibitors of CYP1A2.Except for casiticin the ligands artemisinin and deoxyartemisnin are CYP2C19 inhibitors. Also, spinacetin, deoxyartemisnin and artemisinin are not the inhibitors to CYP2C9, CYP2D6 and CYP3A4 except casiticin. Apigenin, scoparone and kanizol F are not CYP2D6 substrates. Kanizol F are CYP3A4 substrates. Except for apigenin and Kanizol F the scoparone ligands are CYP2C19 inhibitors. Except kanizol F, apigenin, scoparone ligands are not CYP2C9 inhibitors. All the ligands are not the inhibitors to CYP2D6 and CYP3A4.

Table 4.12: Metabolic properties of all selected ligands

S No	Ligands	CYP2D6 substrate	CYP3A4 substrate	CYP1A2 inhibitors	CYP2C19 Inhibitor	CYP2C9 inhibitor	CYP2D6 inhibitor	CYP3A4 inhibitor
1	Afzelechin	No	No	No	No	No	No	No

TABLE 4.12: Metabolic properties of all selected ligands

S No	Ligands	CYP2D6 substrate	CYP3A4 substrate	CYP1A2 inhibitors	CYP2C19 Inhibitor	CYP2C9 inhibitor	CYP2D6 inhibitor	CYP3A4 inhibitor
2	kaempferol	No	No	Yes	No	No	No	No
3	Catechin	No	No	No	No	No	No	No
4	Chrysoplenetin	No	Yes	Yes	Yes	No	No	Yes
5	Arteanniun B	No	Yes	Yes	No	No	No	No
6	Artemisinic acid	No	No	No	No	No	No	No
7	Quercetin	No	No	Yes	No	No	No	No
8	Rutin	No	No	No	No	No	No	No
9	Deoxyartemisnin	No	Yes	Yes	No	No	No	No
10	Casiticin	No	Yes	Yes	Yes	No	No	Yes
11	Spinacetin	No	No	Yes	No	No	No	No
12	Artemisinin	No	Yes	Yes	No	No	No	No
13	Apigenin	No	No	Yes	Yes	No	No	No
14	Scoparone	No	No	Yes	No	No	No	No
15	Kanizol F	No	Yes	No	Yes	Yes	No	No

Some of the parameters of metabolic properties of afzelechin has already been studied by P Bhattachanrya, TN Patel – 2021 [52]. Some parameters of metabolic properties of kaempferol, catechin have been studied by Erman Salih in 2020 [53].

Pkcsm metabolic properties of chrysoplenetin, kanizol F, apigenin and scoparone has already been reported by Zarina Khurshid in 2021 [54].

Some parameters of metabolism of quercetin, rutin, casiticin, spinacetin and artemisinin have been studied by Oluwaseun Taofeek in 2020 [55].

4.6.6 Excretion

The Renal OCT2 substrate acts as a transporter that helps in clearing the drugs and other compounds. Total clearance indicates hepatic clearance which means that drug is metabolized and renal clearance indicates the drug is excreted [54–57].

The excretion values of all selected ligands are given below. Table 4.13 shows the Excretory Properties of all selected ligands.

The table indicates that all these ligands are not renal OCT2 substrates which means the ligands would not be cleared out of the body and hence the total clearance values are given accordingly.

TABLE 4.13: Excretory properties of all selected ligands

S No	Ligands	Total Clearance	Renal OCT 2 Substrate
1	Afzelechin	-0.255	No
2	Kaempferol	0.477	No
3	Catechin	0.183	No
4	Chrysoplenetin	0.627	No
5	Arteanniun B	0.965	No
6	Artemisinic acid	0.639	No
7	Quercetin	0.407	No
8	Rutin	-0.369	No
9	Deoxyartemisnin	0.803	No
10	Casiticin	0.628	No
11	Spinacetin	0.478	No
12	Artemisinin	1.001	No
13	Apigenin	0.566	No
14	Scoparone	0.793	No
15	Kanizol F	0.478	No

Some of the parameters of excretory properties of afzelechin has already been studied by P Bhattacharya, TN Patel in 2021 [52]. Some parameters of excretory properties of kaempferol, catechin have been studied by Erman Salih in 2020 [53]. Pkcsm Excretory properties of apigenin, scoparone, chrysoplenetin has already been reported by Zarina Khurshid in 2021 [54]. Some parameters of excretion properties of casiticin, spinacetin have been studied by Oluwaseun Taofeek in 2020 [55].

4.7 Lead Compound Identification

The physiochemical and the pharmacokinetics properties of the ligands determine their fate as for being drug or non-drug compounds. Lipinski's rule is the first

filter and pharmacokinetics is the second filter for this identification. Rutin does not follow the Lipinski Rule as the Molecular weight, H bond acceptors, and hydrogen bond donor values of Rutin exceed the Lipinski rule, with that Log P-value and Molecular weight. The Log P value of kanizol F is also more than 5 but it is still passed to the next stage. So, in the first stage, only rutin has been knocked out. The next knockout stage is pharmacokinetic screening. In this screening artemisinin and dihydroartemisinic because of being carcinogenic have been knocked out.

Catechin being an hERG II inhibitor has also been knocked out. At the end of this, the compounds left are arteanniun b, deoxyartemisnin, quercetin, scoparone, apigenin, artemetin, artemisinic acid, casiticin, chrysoplenetin. Among all these apigenin and chrysoplenetin are selected as the top two compounds but out of them chrysoplenetin is selected as the lead compound, as much work is already done on apigenin.

4.8 Drug Identification Against HCov-HKU1

At the onset of the disease, numerous FDA-approved medications were repurposed in an endeavor to identify the most efficacious treatment for the virus. Among these medications, remdesivir has been utilized in multiple countries worldwide, including the UK, Brazil, India, Pakistan, and several others.

Despite its increased utilization during the epidemic, Remdesivir is still undergoing clinical trials to ascertain its effectiveness against human coronaviruses [58, 59].

4.8.1 Remdesivir

Remdesivir, an antiviral drug, functions by impeding the replication and spread of viruses akin to coronaviruses within the body. Its primary role is to mitigate the progression of severe symptoms and is employed in the early treatment of HCoV infections [60].

In the treatment of novel coronaviruses like COVID-19 and HCoV, Remdesivir, an FDA-approved antiviral medication overseen by the United States' regulatory body, has been utilized. Remdesivir was initially investigated for its efficacy against Ebola, although those attempts were unsuccessful. This medication, classified as an adenosine analog monophosphoramidate prodrug, exhibits a broad antiviral spectrum, encompassing viruses such as coronaviruses, pneumoviruses, paramyxoviruses, and filoviruses [61].

4.9 Drug ADMET Properties

The drug ADMET properties are studied by using the same software as above which is pkCSM.

4.9.1 Toxicity prediction of Reference Drug

Remdesivir's toxicity properties are given in Table 4.14. Remdesivir's toxicity parameters value indicates that the drug may be detrimental to the liver, while other parameters fall within the range of positive values. This suggests that Remdesivir is not a blocker of hERG I and does not cause skin sensitivity, but inhibitors of hERG II. Additionally, a dosage value of 0.15 is permissible. Consequently, the fact that AMES is not hazardous suggests that it is not carcinogenic.

Table 4.14: Toxicity properties of remdesivir

S.No	Model Name	Predicted Value
1.	AMES Toxicity	No
2.	Max. tolerated dose (human)	0.15
3.	hERG I inhibitor	No
4.	hERG II inhibitor	Yes
5.	Oral rat acute toxicity	2.043
6.	Oral rat chronic toxicity	1.639
7.	Hepatoxicity	Yes
8.	Skin sensitization	No
9.	t.pyriformis toxicity	0.285
10.	Minnow toxicity	0.291

4.9.2 Absorption Properties

Remdesivir's absorption properties are given in Table 4.15. Remdesivir has very low water and $CaCO_2$ solubility, based on the results. Although relatively low, intestinal absorption is still within a suitable range. Its skin permeability value is similarly lower. Remdesivir inhibits P-glycoprotein I and is a substrate of P-glycoprotein; nevertheless, it does not block P-glycoprotein II.

TABLE 4.15: Absorption properties of remdesivir

S. No.	Reference Drug	Remdesivir
1.	Water Solubility	-3.07
2.	CaCO2 Solubility	0.635
3.	Intestinal Absorption (human)	71.109
4.	Skin Permeability	-2.735
5.	P-glycoprotein substrate	Yes
6.	P-glycoprotein I inhibitor	Yes
7.	P-glycoprotein II inhibitor	No

4.9.3 Distribution Properties

The distribution characteristics of Remdesivir is given in Table 4.16. The value of the distribution parameters suggests the drug would not be propagated properly since the value of VDss is low. Remdesivir has the ability to cross the blood-brain barrier and enter the brain's neurological system.

TABLE 4.16: Distribution properties of remdesivir

S. No.	Reference Drug	Remdesivir
1.	VDss (human)	0.307
2.	Fraction unbound (human)	0.005
3.	BBB Permeability	-2.506
4.	CNS Permeability	-4.675

4.9.4 Metabolic Properties

Table 4.17 shows the metabolic properties of remdesivir. It indicates that remdesivir is not a CYP2D6 substrate but it is CYP3A4 substrate. With that table 4.17 shows that remdesivir is not a CYP1A2, CYP2C19, CYP2C9. CYP2D6 and CYP3A4 inhibitor.

TABLE 4.17: Metabolic properties of remdesivir

S. No	Reference Drug	remdesivir
1.	CYP2D6 substrate	No
2.	CYP3A4 substrate	Yes
3.	CYP1A2 inhibitor	No
4.	CYP2C19inhibitor	No
5.	CYP2C9 inhibitor	No
6.	CYP2D6 inhibitor	No
7.	CYP3A4 inhibitor	No

The above table shows the metabolic efficiency of Remdesivir.

4.9.5 Excretion Properties

Table 4.18 shows the excretion properties of remdesivir. The table gives the values of Excretory properties of Remdesivir. It shows that remdesivir is not a renal OCT2 Substrate which means it will not help in clearing of the drug.

With that the value of total clearance as 0.198 is also given with respect to its liver and renal clearance.

TABLE 4.18: Excretion properties of remdesivir

S. No.	Reference Drug	remdesivir
1.	Total Clearance	0.198
2.	Renal OCT2 Substrate	No

4.10 Remdesivir Mechanism of Action

Remdesivir is known to exhibit antiviral activity against several kinds of coronaviruses in vitro, including SARS, MERS, modern human CoV, and bat-CoVs. Remdesivir works by effectively associating with the viral RdRp to induce delay chain termination. Even in circumstances when exonuclease proofreading activity is intact, remdesivir has been shown to interfere with pan-CoV RdRp function by inhibiting the replication of SARS, MERS, and the model β-coronavirus, murine hepatitis virus (MHV) [62].

Remdesivir is often a precursor of a monophosphoramidate nucleoside, which means that it can efficiently move its active metabolite through the cell membrane. Remdesivir monophosphate (RDV-MP), which can avoid an ineffective and rate-limiting initial phosphorylation step, enters target cells and quickly transforms into its active triphosphate form.Remdesivir triphosphate (RDV-TP), which is metabolically active, serves as a substrate for the viral replicase (RdRp) in RNA viruses. Here, it engages in a competitive process with endogenous adenosine triphosphate (ATP) to be incorporated into elongating RNA strands. As shown for the Ebola virus (EBOV), MERS-CoV, SARS-CoV, and SARS-CoV-2, RDV-TP induces delayed chain termination subsequent to its incorporation, resulting in a synthesis arrest. When RDV-TP gets incorporated into SARS-CoV-2, RNA synthesis ceases at three nucleoside/nucleotide sites downstream. Although related analogs of RDV have been under investigation and pharmacological modification for many years [63].

4.11 Remdesivir Effects on the Body

In general, Remdesivir is well absorbed. While there aren't many known adverse consequences, each person and situation will have a different set of dangers. Usually minor and asymptomatic, these liver effects resolve on their own. However, the physician should make sure that everything is okay by maintaining an eye on the liver's health both before and after remdesivir infusions. However, it's not

always evident if remdesivir, COVID-19, or both are to blame for this impact on liver enzymes.

Furthermore, likely are mild to moderate infusion reactions. They are not felt by everyone. If you do, however, they typically occur an hour after your infusion. Certain side effects occur around the injection site, while other side effects spread throughout your body. Symptoms that could exist include: Inflammation or pain where remdesivir was injected, Skin rashes, Changes in blood pressure, Changes in heart rate, Sweating, Fever [64].

4.12 Remdesivir Docking

Table 4.19 shows the docking result of Remdesivir. The table indicates that remdesivir has a binding score of -8.1.

TABLE 4.19: Docking results of remdesivir

Compound	**Binding Score**	**Cavity Size**	**HBD**	**HBA**	**Log P**	**Molecular Weight**	**Rotatable Bonds**	**Grid Map**
Remdesivir	-8.1	4056	4	13	2.31	218602.585	13	-56

The docking results of Remdesivir with Mpro shows that it has quite a good binding score and it has four hydrogen bond donors, and thirteen hydrogen bond acceptors that breaks one of the Lipinski rule .It has thirteen numbers of Rotatable bonds.

4.13 Remdesivir Comparison with Lead Compound

For the reason of assessing bioavailability, safety, effectiveness, and drug-likeness, the lead compound apigenin and the standard medication Remdesivir are compared in terms of their physicochemical and pharmacokinetic properties. Table

4.20 indicates that Remdesivir infringes two of Lipinski's rules: first, regarding molecular weight, as Remdesivir's molecular weight of 602.585 is greater than 500, and second, regarding H-bond acceptor, as Remdesivir accepts 13 hydrogens when Lipinski states that this number should not exceed 10, while chrysoplenetin complies with all of Lipinski's rules regarding LogP, molecular weight, H-bond donor, and H-bond acceptor.

TABLE 4.20: Lipinski Rule Comparison

S No.	**Name of Compound**	**Log P value**	**Molecular Weight g/mol**	**H bond Acceptor**	**H bond Donor**
1.	Remdesivir	2.3121	602.585	13	04
2.	Chrysoplenetin	2.9056	374.3	8	2

4.14 ADMET Properties Comparison

In order to identify a better drug candidate, the absorption, intestinal distribution, metabolic excretion, and toxicity properties of the drug and the lead chemical are assessed using the ADMET properties comparison [63].

4.14.1 Toxicity Comparison

Nine models are employed to evaluate the toxicity of the lead component and the standard medication. According to Model 1 of AMES toxicity, lead and standard chemicals do not cause mutation. According to Model 2 of the Maximum Tolerated Dosage, a number is considered low if it is equal to or less than 0.477 log mg/kg/day, and taken as high if it is larger. The Table below illustrates the low value of the tolerable dosage for apigenin. The third model involves hERG I and II inhibitors, none of which is an inhibitor. The relative toxicity is evaluated using the fourth model of oral rat acute toxicity.

Model 5 of oral rat chronic toxicity provides the lowest dose values that could have an adverse effect. Hepatotoxicity Model 6 suggests that a medicine could damage

the liver. It is clear from the table that remdesivir is toxic to the liver. The number seven is used to verify the dermal goods model's sensitivity to the skin. The lead chemical and the standard are not skin-sensitive. To test for toxicity, Model 8 uses *T. Pyriformis*, while Model 9 uses minnows. Both drugs pass this toxicity test. *T. Pyriformis* value > -0.5 is deemed toxic, meaning remdesivir is fairly hazardous. For minnows, toxicity values below 0.5 mM are considered harmful. The relative toxicity ratings of remdesivir and chrysoplenetin are displayed in Table 4.21.

TABLE 4.21: Toxicity properties comparison

S.No.	Model Name	Remdesivir	Chrysoplenetin
1.	AMES Toxicity	No	No
2.	Max. tolerated dose (human)	0.15	0.491
3.	hERG I inhibitor	No	No
4.	hERG II inhibitor	Yes	No
5.	Oral rat acute toxicity	2.043	2.324
6.	Oral rat chronic toxicity	1.639	1.773
7.	Hepatoxicity	Yes	No
8.	Skin sensitization	No	No
9.	*T.pyriformis* toxicity	0.285	0.313
10.	Minnow toxicity	0.291	2.248

4.14.2 Absorption Properties Comparison

Six models serve as the basis for the absorption parameter. The compound's solubility in water at 25 is indicated by the water solubility model. When a medicine is administered orally, its absorption can be anticipated using the $CaCO_2$ solubility model. High intestine absorption is defined as values larger than 0.90, indicating that chrysoplenetin is absorbed more than remdesivir. Less than 30% on the intestinal absorption model is regarded as insufficient absorption. The findings for the lead and standard compounds show chrysoplenetin has a high intestine rate of absorption. The two compounds pass the skin penetration test for transdermal medicines, as shown by the skin permeability model, which considers values less than log Kp > -2.5 to be low. P-glycoprotein's substrate model is extremely poorly absorbed. Because P-glycoprotein serves as a biological barrier and an

ABC transporter, the P-glycoprotein substrate model is important. Remdesivir and chrysoplenetin act as the substrates.

TABLE 4.22: Absorption properties comparison

S. No.	Reference drug	Remdesivir	Chrysoplenetin
1.	Water Solubility	-3.07	-3.605
2.	CaCO2 Solubility	0.635	1.393
3.	Intestinal Absorption (human)	71.109	99.856
4.	Skin Permeability	-2.735	-2.743
5.	P-glycoprotein substrate	Yes	Yes
6.	P-glycoprotein I inhibitor	Yes	No
7.	P-glycoprotein II inhibitor	No	Yes
8.	Skin sensitization	No	No
9.	t.pyriformis toxicity	0.285	0.313
10.	Minnow toxicity	0.291	2.248

4.14.3 Metabolic Properties Comparison

Mostly found in the liver, cytochrome P450 is an enzyme responsible for detoxification as it oxidizes foreign substances and renders them easier for the body to be eliminated. It either deactivates or activates some medicines. Understanding whether a chemical is a P450 substrate or not, as well as if it is an inhibitor of P450, is crucial. Table 4.23 shows that whilst chrysoplenetin is a CYP3A4 substrate, it is also an inhibitor of CYP1A2, CYP2C19, and CYP3A4. Remdesivir is a CYP3A4 substrate.

TABLE 4.23: Metabolic properties comparison

S. No.	Reference Drug	Remdesivir	Chrysoplenetin
1.	CYP2D6 substrate	No	No
2.	CYP3A4 substrate	Yes	Yes
3.	CYP1A2 inhibitor	No	Yes
4.	CYP2C19 inhibitor	No	Yes
5.	CYP2C9 inhibitor	No	No
6.	CYP2D6 inhibitor	No	No
7.	CYP3A4 inhibitor	No	Yes
8.	Skin sensitization	No	No
9.	t.pyriformis toxicity	0.285	0.313

TABLE 4.23: Metabolic properties comparison

S. No.	Reference Drug	Remdesivir	Chrysoplenetin
10.	Minnow toxicity	0.291	2.248

4.14.4 Distribution Properties Comparison

The dispersion features of Remdesivir and Chrysoplenetin are contrasted in Table 4.24. Four models serve as a basis for the distribution parameter. The medication's uniform distribution in blood plasma is determined by the volume of distribution (VDss); if the value is more than 2.81 L/kg, the drug is more evenly distributed in the tissues than in the blood plasma. Chrysoplenetin and Remdesivir both have a respectable VDss value. The second model is predicated on the proportion of medicines in plasma that are unbound, as medications that are bounded have an impact on drug efficiency. The amount of medicine that is still unbounded is indicated by the provided value.

When a drug's BBB permeability value reaches 0.3 logBB, it can readily pass across the blood-brain barriers; moreover, the medicine is not or is not delivered to the brain well enough if the value is less than -1 logBB. These numbers make it obvious that Remdesivir has a low value, which means the brain would not get enough of it. In contrast, the central nervous system (CNS) model depends on the idea that drugs with a logPS value more than -2 may readily enter the CNS, but drugs with a logPS value less than -3 are unable to reach the CNS. Remdesivir is unable to travel through the central nervous system due to its low value.

TABLE 4.24: Distribution properties comparison

S. No.	Reference Drug	Remdesivir	Chrysoplenetin
1.	VDss (human)	0.307	-0.161
2.	Fraction unbound (human)	0.005	0.103
3.	BBB Permeability	-2.056	-1.043
4.	CNS Permeability	-4.675	-3.226

4.14.5 Excretion Properties Comparison

In order to assess the medication dosage rates, the total clearance value—which includes hepatic and renal clearance—is essential. Remdesivir has less overall clearance than chystoplenitin. The renal OCT2 (organic cation transporter 2) model is the second one, and it aids in the renal clearance of medications and other substances. In respect to inhibitors, one could suffer adverse reactions from being an OCT2 substrate. Therefore, neither Remdesivir nor Chrysoplenetin are substrates of Renal OCT2. The excretory features of Remdesivir and Chrysoplenetin are shown in Table 4.25.

TABLE 4.25: Excretion properties comparison

S. No.	Reference Drug	Remdesivir	Chrysoplenetin
1.	Total Clearance	0.198	0.627
2.	Renal OCT2 Substrate	No	No

4.15 Physiochemical Properties Comparison

The physiochemical properties of the compounds are examined in order to ascertain their fundamental properties. Remdesivir contains 27 carbon atoms, 35 hydrogen atoms, 6 nitrogen atoms, 8 oxygen atoms, and 1 phosphorus atom, according to this screening, whereas chrysoplenetin has 19 carbon atoms, 18 hydrogen atoms, and 8 oxygen atoms. In accordance with this, apigenin is a fundamental biological molecule that is associated with Remdesivir. Chrysoplenetin is able to provide two hydrogen atoms, showing the oxidation state, whereas remdesivir can donate four hydrogen atoms, thirteen hydrogen atoms that do not violate the Lipinski rule can be absorbed by remdesivir. Remdesivir does not meet the Lipinski rule and has a molecular weight that is significantly greater than chrysoplenetin, although having a lower Log P value. Considering the number of rotatable bonds, Remdesivir has thirteen, whereas chrysoplenetin has just five. The physiological and chemical features of remdesivir and chrysoplenetin are examined in Table 4.26.

TABLE 4.26: Physiochemical properties comparison

S No.	Drug	Mol. Formula	HBA	HBD	Log P	Mol. Formula	Rotatable Bonds
1.	Remdesivir	$C_{27}H_{35}N_6O_8P$	13	4	2.31218	602.585	13
2.	Chrysoplenetin	$C_{19}H_{18}O_8$	2	8	2.9056	374.3	5

4.16 Docking Score Comparison

We docked the standard and the lead compound against the Mpro, and the best binding score was determined from the docking result. As Table 4.27 indicates, the vina score of the lead chemical, Chrysoplenetin, is lower than that of Remdesivir, the standard medication.

Remdesivir and Chrysoplenetin had binding scores of -8.1 and -7.9, accordingly, which are higher than those of the prescribed drugs. The result suggests that chrysoplenetin is able to bind or prevent Mpro more effectively than Remdesivir.

TABLE 4.27: Docking score comparison

S.No.	**Compound**	**Binding Score**
1.	Remdesivir	-8.1
2.	Chrysoplenetin	-7.9

4.17 Docking Analysis Comparison

The docking results are analyzed by LigPlot based on the number of hydrogen bonds, number of hydrophobic interactions, number of interacting amino acids, and that of steric interactions. Figure 4.19 and 4.20 shows the docking results of remdesivir and chrysoplenetin. Figure 4.19 shows that remdesivir has formed only five hydrogen bond and eleven hydrophobic interactions.

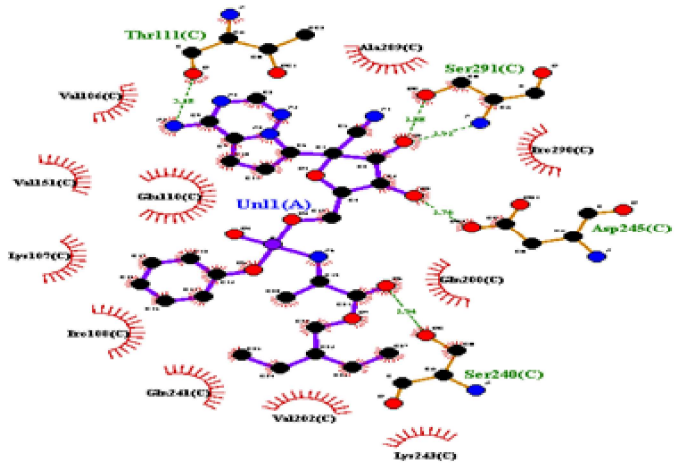

FIGURE 4.19: Interaction of remdesivir with the receptor

Figure 4.20 shows that chrysoplenetin has formed five hydrogen bonds and nine hydrophobic interactions.

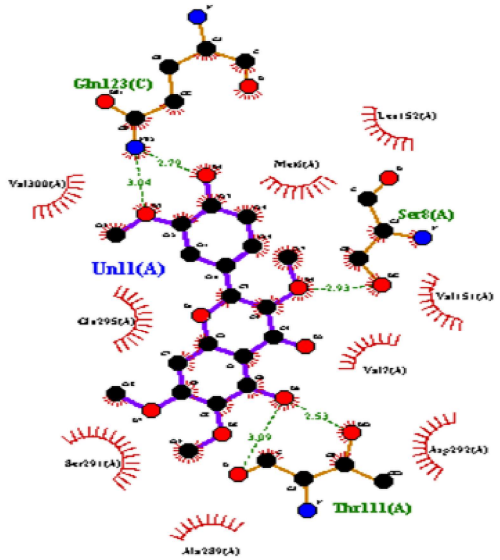

FIGURE 4.20: Interaction of chrysoplenetin with receptor

The details of hydrogen and hydrophobic interactions are mentioned in the Table 4.28. chrysoplenetin forms five hydrogen bonds whereas remdesivir form five hydrogen bond, this is mainly because chrysoplenetin O2, O4, O5, O6, O7, and O8 has made interactions with the receptor. Remdesivir makes 11 hydrophobic

interactions whereas chrysoplenetin makes 9 of them. With all this information chrysoplenetin succeeds to be much better than Remdesivir.

TABLE 4.28: Docking analysis comparison

S. No	Ligand Name	Binding Energy	No. of HB	Hydrogen Bond Amino acids	Hydrogen Bond Distance	Hydrophobic Bonding
1	Remdesivir	-8.1	5	O-Ser291-CO	3.94	Lys 243
				N-Ser291-O	2.93	Gln 200
				OC-Ser240-O	3.13	Val 202
				O-Thr111-N	3.76	Gln 241
				O-Asp245-OC	2.33	Pro 108
						Lys 107
						Val 151
						Gln110
						Pro290
						Val106
						Ala289
2	Chrysoplenetin	-7.9	5	OG1-Thr111-O6	2.72	Leu 152
				O-Thr111-O6	3.04	Met 6
				N-Gln123-O	3.09	Val 151
				O-Gln123-N	2.52	Val 7
				OG-Ser8-N	2.93	Asp 292
						Ala 289
						Ser 291
						Gln 295
						Val 300

The above table 4.28 shows that Ala 289, Val 106, Val 151, Gln 110, Pro 108, Lys 107 Lys 243, Gln 200, Pro 290 participates in forming hydrophobic interaction between the protein and Remdesivir . Whereas Val 300 , Gln 295 ,Ser 291 ,Ala 289, Asp 292 Val 7 ,Val 151 , Met 6 and Leu 152 forming hydrophobic interaction between the protein and chrysoplenetin.

Chapter 5

Conclusion and Future Prospects

The study aimed to determine active constituents in the plant *Artemisia absinthium* which is also known as Common wormwood in common language. For this purpose, 15 ligands were selected to be docked against the main protease of coronavirus. The structure of all the 15 ligands was easily available in PubChem and protein structure was also available in PDB. All the ligands were docked against the receptor protein via CB Dock. The results were visualized using PyMol and were analyzed through LigPlot. Out of those 15 ligands, Rutin was first screened out based on Lipinski's rule, and based on second screening Artemisinin, Dihydroartemisinic, were knocked out. After these 13 ligands were left and out of those Chrysoplenetin and Apigenin were the two best active ligands. Based on the hydrophobic and hydrogen bonding Chrysoplenetin was selected as a lead against the standard drug Remdesivir which is in use for the treatment of this virus. With the final results, it was cleared that Chrysoplenetin can bind far better to M^{pro} than that of Remdesivir.

5.1 Recommendations

As per the findings of this research chrysoplenetin should be exploited more against HCoV-HKu1. With this other active constituent like apigenin, quercetin,

artemisinic acid, deoxyartemisnin, casiticin and apigenin have also shown a positive result in response to M^{pro}. Previously, *Artemisia absinthium* has been used as anti-viral, anti-inflammatory, anti-oxidants, and anti-malarial for this reason *Artemisia absinthium* should be explored more for its effectiveness against HCoV-HKU1.

Bibliography

[1] Y. X. Lim, Y. L. Ng, J. P. Tam, and D. X. Liu, "Human coronaviruses: a review of virus–host interactions," *Diseases*, vol. 4, no. 3, p. 26, 2016.

[2] P. C. Woo, S. K. Lau, C.-m. Chu, K.-h. Chan, H.-w. Tsoi, Y. Huang, B. H. Wong, R. W. Poon, J. J. Cai, W.-k. Luk *et al.*, "Characterization and complete genome sequence of a novel coronavirus, coronavirus hku1, from patients with pneumonia," *Journal of virology*, vol. 79, no. 2, pp. 884–895, 2005.

[3] H. D. Davies, A. Matlow, M. Petric, R. Glazier, and E. E. Wang, "Prospective comparative study of viral, bacterial and atypical organisms identified in pneumonia and bronchiolitis in hospitalized canadian infants," *The Pediatric infectious disease journal*, vol. 15, no. 4, pp. 371–375, 1996.

[4] D. X. Liu, J. Q. Liang, and T. S. Fung, "Human coronavirus-229e,-oc43,-nl63, and-hku1 (coronaviridae)," *Encyclopedia of virology*, p. 428, 2021.

[5] X. Li, H. K. Luk, S. K. Lau, and P. C. Woo, "Human coronaviruses: general features," *Reference module in biomedical sciences*, 2019.

[6] i. Andrew J. Broadbent, Kanta Subbarao, "Human coronavirus 229e - an overview — sciencedirect topics," https://www.sciencedirect.com/topics/veterinary-science-and-veterinary-medicine/human-coronavirus-229e, (Accessed on 02/03/2024).

[7] P. Hunziker, "Vaccination strategies for minimizing loss of life in covid-19 in a europe lacking vaccines," *MedRxiv*, pp. 2021–01, 2021.

[8] M. F. Boni, P. Lemey, X. Jiang, T. T.-Y. Lam, B. W. Perry, T. A. Castoe, A. Rambaut, and D. L. Robertson, "Evolutionary origins of the sars-cov-2

sarbecovirus lineage responsible for the covid-19 pandemic," *Nature microbiology*, vol. 5, no. 11, pp. 1408–1417, 2020.

[9] Y. Chen, Q. Liu, and D. Guo, "Emerging coronaviruses: genome structure, replication, and pathogenesis," *Journal of medical virology*, vol. 92, no. 4, pp. 418–423, 2020.

[10] N. Zhu, D. Zhang, W. Wang, X. Li, B. Yang, J. Song, X. Zhao, B. Huang, W. Shi, R. Lu *et al.*, "A novel coronavirus from patients with pneumonia in china, 2019," *New England journal of medicine*, vol. 382, no. 8, pp. 727–733, 2020.

[11] Q. Zhao, S. Li, F. Xue, Y. Zou, C. Chen, M. Bartlam, and Z. Rao, "Structure of the main protease from a global infectious human coronavirus, hcov-hku1," *Journal of virology*, vol. 82, no. 17, pp. 8647–8655, 2008.

[12] P. C. Woo, S. K. Lau, C. C. Yip, Y. Huang, and K.-Y. Yuen, "More and more coronaviruses: human coronavirus hku1," *Viruses*, vol. 1, no. 1, pp. 57–71, 2009.

[13] K. Pyrc, B. Berkhout, and L. van der Hoek, "The novel human coronaviruses nl63 and hku1," *Journal of virology*, vol. 81, no. 7, pp. 3051–3057, 2007.

[14] K. Pyrc, A. C. Sims, R. Dijkman, M. Jebbink, C. Long, D. Deming, E. Donaldson, A. Vabret, R. Baric, L. van der Hoek *et al.*, "Culturing the unculturable: human coronavirus hku1 infects, replicates, and produces progeny virions in human ciliated airway epithelial cell cultures," *Journal of virology*, vol. 84, no. 21, pp. 11 255–11 263, 2010.

[15] D. X. Liu, J. Q. Liang, and T. S. Fung, "Human coronavirus-229e,-oc43,-nl63, and-hku1 (coronaviridae)," *Encyclopedia of virology*, p. 428, 2021.

[16] N. Friedman, H. Alter, M. Hindiyeh, E. Mendelson, Y. Shemer Avni, and M. Mandelboim, "Human coronavirus infections in israel: epidemiology, clinical symptoms and summer seasonality of hcov-hku1," *Viruses*, vol. 10, no. 10, p. 515, 2018.

[17] SinoBiological, "Coronavirus treatment — sino biological," https://www.sinobiological.com/research/virus/coronavirus-treatment, (Accessed on 02/03/2024).

[18] R. Mann, A. Perisetti, M. Gajendran, Z. Gandhi, C. Umapathy, and H. Goyal, "Clinical characteristics, diagnosis, and treatment of major coronavirus outbreaks," *Frontiers in medicine*, vol. 7, p. 581521, 2020.

[19] B. Benarba and A. Pandiella, "Medicinal plants as sources of active molecules against covid-19," *Frontiers in pharmacology*, vol. 11, p. 1189, 2020.

[20] S. Ćavar, M. Maksimović, D. Vidic, and A. Parić, "Chemical composition and antioxidant and antimicrobial activity of essential oil of artemisia annua l. from bosnia," *Industrial crops and products*, vol. 37, no. 1, pp. 479–485, 2012.

[21] K.-M. Li, X. Dong, Y.-N. Ma, Z.-H. Wu, Y.-M. Yan, and Y.-X. Cheng, "Antifungal coumarins and lignans from artemisia annua," *Fitoterapia*, vol. 134, pp. 323–328, 2019.

[22] A. Septembre-Malaterre, M. Lalarizo Rakoto, C. Marodon, Y. Bedoui, J. Nakab, E. Simon, L. Hoarau, S. Savriama, D. Strasberg, P. Guiraud *et al.*, "Artemisia annua, a traditional plant brought to light," *International journal of molecular sciences*, vol. 21, no. 14, p. 4986, 2020.

[23] C. J. Morris and D. D. Corte, "Using molecular docking and molecular dynamics to investigate protein-ligand interactions," *Modern Physics Letters B*, vol. 35, no. 08, p. 2130002, 2021.

[24] L. Zhang, D. Lin, X. Sun, U. Curth, C. Drosten, L. Sauerhering, S. Becker, K. Rox, and R. Hilgenfeld, "Crystal structure of sars-cov-2 main protease provides a basis for design of improved α-ketoamide inhibitors," *Science*, vol. 368, no. 6489, pp. 409–412, 2020.

[25] S. G. Kshirsagar and R. V. Rao, "Antiviral and immunomodulation effects of artemisia," *Medicina*, vol. 57, no. 3, p. 217, 2021.

[26] J. Zhou, G. Xie, and X. Yan, "Encyclopedia of traditional chinese medicines," *Isolat Compound AB*, vol. 1, p. 455, 2011.

[27] J. He, L. Hu, X. Huang, C. Wang, Z. Zhang, Y. Wang, D. Zhang, and W. Ye, "Potential of coronavirus 3c-like protease inhibitors for the development of new anti-sars-cov-2 drugs: Insights from structures of protease and inhibitors," *International journal of antimicrobial agents*, vol. 56, no. 2, p. 106055, 2020.

[28] T. Madej, C. J. Lanczycki, D. Zhang, P. A. Thiessen, R. C. Geer, A. Marchler-Bauer, and S. H. Bryant, "Mmdb and vast+: tracking structural similarities between macromolecular complexes," *Nucleic acids research*, vol. 42, no. D1, pp. D297–D303, 2014.

[29] N. S. Pagadala, K. Syed, and J. Tuszynski, "Software for molecular docking: a review," *Biophysical reviews*, vol. 9, pp. 91–102, 2017.

[30] F. Wu, S. Zhao, B. Yu, Y.-M. Chen, W. Wang, Z.-G. Song, Y. Hu, Z.-W. Tao, J.-H. Tian, Y.-Y. Pei *et al.*, "Author correction: A new coronavirus associated with human respiratory disease in china," *Nature*, vol. 580, no. 7803, p. E7, 2020.

[31] M. R. Macnaughton, "Occurrence and frequency of coronavirus infections in humans as determined by enzyme-linked immunosorbent assay," *Infection and Immunity*, vol. 38, no. 2, pp. 419–423, 1982.

[32] R. Dias, J. de Azevedo, and F. Walter, "Molecular docking algorithms," *Current drug targets*, vol. 9, no. 12, pp. 1040–1047, 2008.

[33] W. L. DeLano *et al.*, "Pymol: An open-source molecular graphics tool," *CCP4 Newsl. Protein Crystallogr*, vol. 40, no. 1, pp. 82–92, 2002.

[34] S. Yuan, H. S. Chan, and Z. Hu, "Using pymol as a platform for computational drug design," *Wiley Interdisciplinary Reviews: Computational Molecular Science*, vol. 7, no. 2, p. e1298, 2017.

[35] S. Farabi, N. R. Saha, N. A. Khan, and M. Hasanuzzaman, "Prediction of sars-cov-2 main protease inhibitors from several medicinal plant compounds by drug repurposing and molecular docking approach." 2020.

[36] B. Russell, C. Moss, G. George, A. Santaolalla, A. Cope, S. Papa, and M. Van Hemelrijck, "Associations between immune-suppressive and stimulating drugs and novel covid-19—a systematic review of current evidence," *ecancermedicalscience*, vol. 14, 2020.

[37] T. P. Sheahan, A. C. Sims, S. R. Leist, A. Schäfer, J. Won, A. J. Brown, S. A. Montgomery, A. Hogg, D. Babusis, M. O. Clarke *et al.*, "Comparative therapeutic efficacy of remdesivir and combination lopinavir, ritonavir, and interferon beta against mers-cov," *Nature communications*, vol. 11, no. 1, p. 222, 2020.

[38] M. L. Holshue, C. DeBolt, S. Lindquist, K. H. Lofy, J. Wiesman, H. Bruce, C. Spitters, K. Ericson, S. Wilkerson, A. Tural *et al.*, "First case of 2019 novel coronavirus in the united states," *New England journal of medicine*, vol. 382, no. 10, pp. 929–936, 2020.

[39] N. S. Pagadala, K. Syed, and J. Tuszynski, "Software for molecular docking: a review," *Biophysical reviews*, vol. 9, pp. 91–102, 2017.

[40] S. Hunter, P. Jones, A. Mitchell, R. Apweiler, T. K. Attwood, A. Bateman, T. Bernard, D. Binns, P. Bork, S. Burge *et al.*, "Interpro in 2011: new developments in the family and domain prediction database," *Nucleic acids research*, vol. 40, no. D1, pp. D306–D312, 2012.

[41] E. Yuriev, J. Holien, and P. A. Ramsland, "Improvements, trends, and new ideas in molecular docking: 2012–2013 in review," *Journal of Molecular Recognition*, vol. 28, no. 10, pp. 581–604, 2015.

[42] R. Dias, J. de Azevedo, and F. Walter, "Molecular docking algorithms," *Current drug targets*, vol. 9, no. 12, pp. 1040–1047, 2008.

[43] S. I. Mostafa, "Mixed ligand complexes with 2-piperidine-carboxylic acid as primary ligand and ethylene diamine, 2, 2'-bipyridyl, 1, 10-phenanthroline

and 2 (2'-pyridyl) quinoxaline as secondary ligands: preparation, characterization and biological activity," *Transition Metal Chemistry*, vol. 32, no. 6, pp. 769–775, 2007.

[44] S. Farabi, N. R. Saha, N. A. Khan, and M. Hasanuzzaman, "Prediction of sars-cov-2 main protease inhibitors from several medicinal plant compounds by drug repurposing and molecular docking approach." 2020.

[45] B. Russell, C. Moss, G. George, A. Santaolalla, A. Cope, S. Papa, and M. Van Hemelrijck, "Associations between immune-suppressive and stimulating drugs and novel covid-19—a systematic review of current evidence," *ecancermedicalscience*, vol. 14, 2020.

[46] T. P. Sheahan, A. C. Sims, S. R. Leist, A. Schäfer, J. Won, A. J. Brown, S. A. Montgomery, A. Hogg, D. Babusis, M. O. Clarke *et al.*, "Comparative therapeutic efficacy of remdesivir and combination lopinavir, ritonavir, and interferon beta against mers-cov," *Nature communications*, vol. 11, no. 1, p. 222, 2020.

[47] M. L. Holshue, C. DeBolt, S. Lindquist, K. H. Lofy, J. Wiesman, H. Bruce, C. Spitters, K. Ericson, S. Wilkerson, A. Tural *et al.*, "First case of 2019 novel coronavirus in the united states," *New England journal of medicine*, vol. 382, no. 10, pp. 929–936, 2020.

[48] D. Niemeyer, K. Mösbauer, E. M. Klein, A. Sieberg, R. C. Mettelman, A. M. Mielech, R. Dijkman, S. C. Baker, C. Drosten, and M. A. Müller, "The papain-like protease determines a virulence trait that varies among members of the sars-coronavirus species," *PLoS pathogens*, vol. 14, no. 9, p. e1007296, 2018.

[49] K. Y. Wang, F. Liu, R. Jiang, X. Yang, T. You, X. Liu, C. Q. Xiao, Z. Shi, H. Jiang, Z. Rao *et al.*, "Structure of mpro from covid-19 virus and discovery of its inhibitors," *Nature*, vol. 582, no. 7811, pp. 289–93, 2020.

[50] V. K. Morya, S. Yadav, E.-K. Kim, and D. Yadav, "In silico characterization of alkaline proteases from different species of aspergillus," *Applied biochemistry and biotechnology*, vol. 166, pp. 243–257, 2012.

[51] C. Wu, Y. Liu, Y. Yang, P. Zhang, W. Zhong, Y. Wang, Q. Wang, Y. Xu, M. Li, X. Li *et al.*, "Analysis of therapeutic targets for sars-cov-2 and discovery of potential drugs by computational methods," *Acta Pharmaceutica Sinica B*, vol. 10, no. 5, pp. 766–788, 2020.

[52] P. Bhattacharya and T. N. Patel, "Deregulation of mmr-related pathways and anticancer potential of curcuma derivatives–a computational approach," 2021.

[53] E. S. Istifli, A. Ş. Tepe, C. SarikÜrkcÜ, and B. Tepe, "Interaction of certain monoterpenoid hydrocarbons with the receptor binding domain of 2019 novel coronavirus (2019-ncov), transmembrane serine protease 2 (tmprss2), cathepsin b, and cathepsin l (catb/l) and their pharmacokinetic properties," *Turkish Journal of Biology*, vol. 44, no. 7, pp. 242–264, 2020.

[54] E. Irfan, "Screening of active constituents of artemisia annua against viral main protease m pro/clpro of sars-cov-2–an insilico study," Ph.D. dissertation, CAPITAL UNIVERSITY, 2021.

[55] O. TAOFEEK, "Molecular docking and admet analyses of photochemicals from nigella sativa (blackseed), trigonella foenum-graecum (fenugreek) and anona muricata (soursop) on sars-cov-2 target," *ScienceOpen Preprints*, 2020.

[56] M. Sankar, B. Ramachandran, B. Pandi, N. Mutharasappan, V. Ramasamy, P. G. Prabu, G. Shanmugaraj, Y. Wang, B. Muniyandai, S. Rathinasamy *et al.*, "In silico screening of natural phytocompounds towards identification of potential lead compounds to treat covid-19," *Frontiers in molecular biosciences*, vol. 8, p. 637122, 2021.

[57] B. Yabrir, A. Belhassan, T. Lakhlifi, G. Salgado M, M. Bouachrine, P. Munoz C, L. Gerli C, and R. Ramirez T, "Minor composition compounds of algerian herbal medicines as inhibitors of sars-cov-2 main protease: Molecular docking and admet properties prediction," *Journal of the Chilean Chemical Society*, vol. 66, no. 1, pp. 5067–5074, 2021.

[58] K. C. Badgujar, A. H. Ram, R. Zanznay, H. Kadam, and V. C. Badgujar, "Remdesivir for covid-19: A review of pharmacology, mechanism of action,

in-vitro activity and clinical use based on available case studies," *Journal of Drug Delivery and Therapeutics*, vol. 10, no. 4-s, pp. 264–270, 2020.

[59] ——, "Remdesivir for covid-19: A review of pharmacology, mechanism of action, in-vitro activity and clinical use based on available case studies," *Journal of Drug Delivery and Therapeutics*, vol. 10, no. 4-s, pp. 264–270, 2020.

[60] NHS, "About remdesivir - nhs," https://www.nhs.uk/medicines/remdesivir-veklury/about-remdesivir/, (Accessed on 02/03/2024).

[61] T. C. P. d. Azevedo, P. C. P. d. Azevedo, R. N. Silveira Filho, A. R. V. S. d. Carvalho, M. L. Cezarotti Filho, F. T. Barbosa, C. F. d. Sousa-Rodrigues, T. J. Matos-Rocha, and F. W. d. S. Ramos, "Use of remdesivir for patients with covid-19: a review article," *Revista da Associação Médica Brasileira*, vol. 66, pp. 838–841, 2020.

[62] R. T. Eastman, J. S. Roth, K. R. Brimacombe, A. Simeonov, M. Shen, S. Patnaik, and M. D. Hall, "Remdesivir: a review of its discovery and development leading to emergency use authorization for treatment of covid-19," *ACS central science*, vol. 6, no. 5, pp. 672–683, 2020.

[63] A. Simonis, S. J. Theobald, G. Fätkenheuer, J. Rybniker, and J. J. Malin, "A comparative analysis of remdesivir and other repurposed antivirals against sars-cov-2," *EMBO molecular medicine*, vol. 13, no. 1, p. e13105, 2021.

[64] J. Murdock, "Here are remdesivir's possible side effects (intravenous injection) - goodrx," https://www.goodrx.com/remdesivir/remdesivir-side-effects, (Accessed on 02/03/2024).